What makes forests escape wildfire:

A study of Chornobyl Exclusion Zone (ChEZ), Ukraine

Amal Anil Kumar Lathika Amma

Master thesis • 30 credits
Swedish University of Agricultural Sciences, SLU
Southern Swedish Forest Research Centre
Sustainable Nature and Forest Management (SUFONAMA)
Alnarp 2024

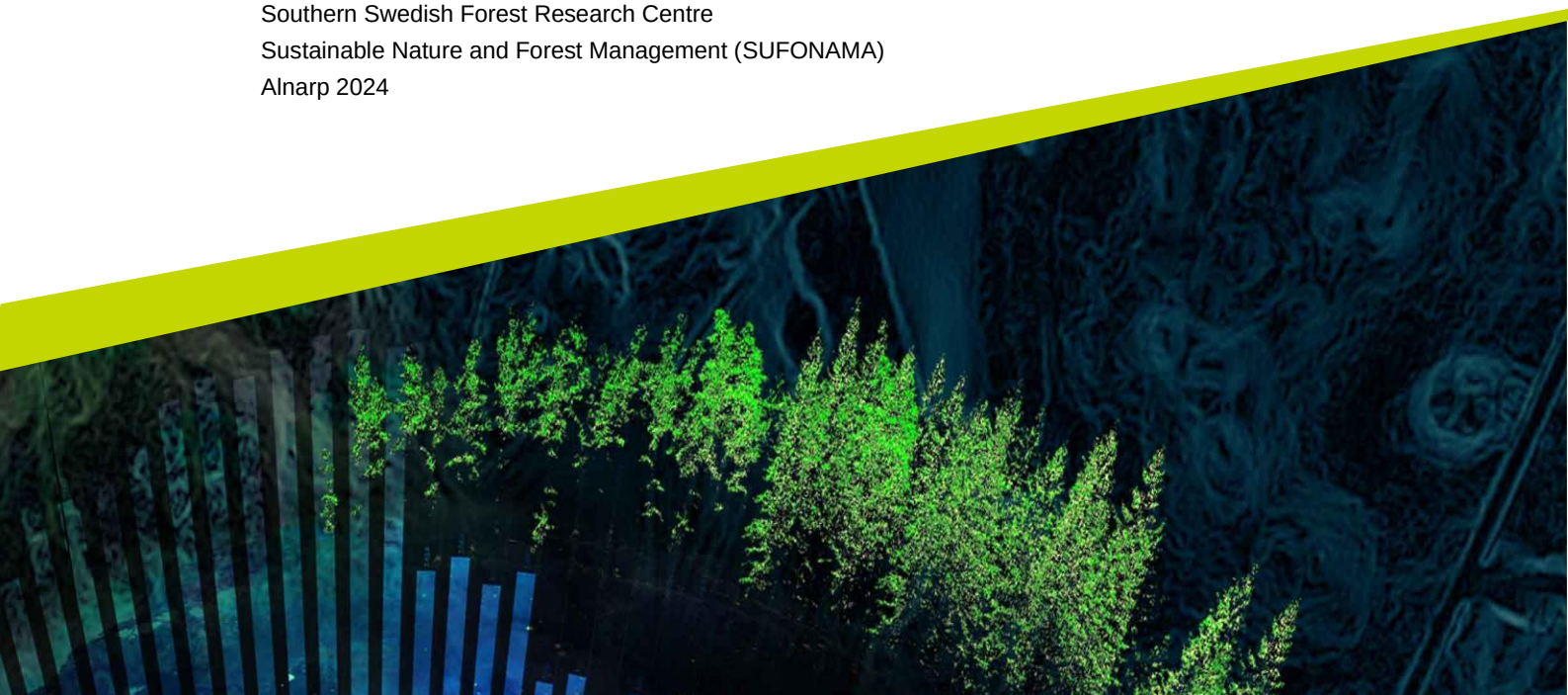

What makes forests escape wildfires: A study of Chornobyl Exclusion Zone (ChEZ), Ukraine

Vilka beståndsegenskaper hjälper skogar undkomma naturliga bränder: en studie i Chornobyl Exclusion Zone, Ukraina

Amal Anil Kumar Lathika Amma

Supervisor:	**Dr Maksym Matsala, Swedish University of Agricultural Sciences, Southern Swedish Forest Research Centre**
Assistant supervisor:	Dr Igor Drobyshev, Swedish University of Agricultural Sciences, Southern Swedish Forest Research Centre
Examiner:	Renat Trubins, Swedish University of Agricultural Sciences, Southern Swedish Forest Research Centre

Credits:	30 credits
Level:	Second cycle, A2E
Course title:	Master's Thesis in Forest Science
Course code:	EX0984
Programme/Education:	Master’s program in Sustainable Forest and Nature Management (SUFONAMA)
Course coordinating dept:	Southern Swedish Forest Research Centre
Place of publication:	Alnarp
Year of publication:	2024
Copyright:	All featured images are used with permission from the copyright owner.
Keywords:	Broadleaves, Chornobyl Exclusion Zone, classification models, forest fire, fuel, presence of broadleaves, Random Forest, refugia occurrence, Remote sensing

Swedish University of Agricultural Sciences
Faculty of Forest Sciences
Southern Swedish Forest Research Centre

Abstract

In May 2022, there was a mega-fire in the south-eastern part of ChEZ, caused by the Russian Invasion of Ukraine. It burned plantations established after the mega-fire in 1992 in the same area. Despite the mega-fire, some forest patches survived. A detailed analysis of forest management data from 2016 shows that the survived forest patches were comprised of broadleaved tree species with more than 80% of the canopy. This suggests that the dominance of broadleaves could be the factor that contributed to the survival of the forest patches (refugia). Consequently, this study investigates the characteristics of their surrounding forests that enhance the likelihood of these forests escaping large natural fires. We hypothesize that fuel discontinuity and structural heterogeneity in the buffers increase the probability of refugia occurrence. We used available local forest inventory datasets (geospatial polygons with attribute tables) from 2016 to map fire refugia and their adjacent areas (buffer zones) using QGIS and R. From the GEDI LiDAR footprints and Planet satellite images that were acquired before (2021) and after the mega-fire, we created wall-to-wall maps for canopy cover (CC), canopy height (CH), presence of broadleaves (POB) and forest cover (FC). Spectral bands were used as the predictor variables for predicting these attributes. CC map was used as a proxy for fuel discontinuity, and the POB map was used as a proxy for fuel type. We extracted the values of the variables from the maps for 10 m, 30 m, and 50 m buffers around survived and burned polygons. CH difference was calculated as the difference in CH between buffer and polygon, which was used as a proxy for structural heterogeneity. Using these variables as predictors, we developed Random Forest models for the 10 m, 30 m, and 50 m buffers that predict refugia occurrence using R. After analyzing the refugia occurrence with variable importance plots and partial dependence plots, we found that the fuel type, POB was the factor that saved some forests from the 2022 mega-fire. We could not find any evidence to support our hypothesis of structural heterogeneity and fuel discontinuity. It was observed that the decrease in the probability of refugia occurrence despite higher POB values was due to the adjacence of the non-refugia buffers to highly flammable Scots pine stands. These stands got burned, and the crown fire spread to surrounding patches and burned them down even if the POB values ranged between 75-81.5% in their buffers of 10 m width. This research recommends incorporating broadleaved species such as European oak, European aspen, and silver birch into the future production forest management regimes as they are fire-resistant and enhance forest resilience.

Keywords: Broadleaves, Chornobyl Exclusion Zone, classification models, forest fire, fuel, presence of broadleaves, Random Forest, refugia occurrence, Remote sensing

Table of contents

List of tables

List of figures

Abbreviations

^{90}Sr	Strontium-90
^{137}Cs	Caesium-137
^{237}Np	Neptunium-237
$^{238\text{-}240}Pu$	Plutonium-238, Plutonium-239, Plutonium-240
^{241}Am	Americium-241
CC	Canopy Cover
CH	Canopy Height
CH_4	Methane
ChEZ	Chornobyl Exclusion Zone
CO_2	Carbon dioxide
dNBR	delta Normalized Burn Ratio
dNDVI	delta Normalized Difference Vegetation Index
FC	Forest Cover
GAM	Generalized Additive Model
GEDI	Global Environmental Development Investigation
GSV	Growing Stock Volume
ISS	International Space Station
LiDAR	Light Detection and Ranging
MODIS	Moderate Resolution Imaging Spectroradiometer
MSE	Mean Square Error
NA	Not Available
NASA	National Aeronautics and Space Administration
N_2O	Nitrous Oxide
NIR	Near Infra-Red
OOB	Out-Of-Bag
PAR	Photosynthetically Active Radiation
PER	Polesie State Radioecological Reserve
POB	Presence Of Broadleaves

QGIS	Quantum Geographical Information System
RF	Random Forest
RH	Relative Height
RMSE	Root Mean Square Error
SWIR	Short Wave Infra-Red
$T_{1/2}$	Half-life
TIR	Thermal Infra-Red
UAV	Unmanned Aerial Vehicle

1. Introduction

1.1 Fire ecology and forest fuels

Wildfires have shaped terrestrial ecosystem dynamics worldwide (Bowman *et al.*, 2009; Jones et al., 2022). Fire is crucial in the carbon cycle, floral and faunal distribution, and nutrient cycling (Collins *et al.*, 2019b; Flannigan, Stocks, and Wotton, 2000). Forest fires have impacted the global carbon cycle for ~420 million years (Sommers, Loehman, and Hardy, 2014). The complex interactions between vegetation fuels, topography, and weather drive the behavior of forest fires (Agee, 1993; Bradstock et al., 2010; Meddens et al., 2018; Meigs & Krawchuk, 2018).

Unmanaged forests are characterized by three-dimensional, dense fuel patches with varying sizes, amounts, and spatial arrangements, creating conditions ripe for fire (Agee, 1993). They accumulate many combustible, dry deadwood, litter, and parched, dead trees, which are significant fuel sources in the forest. As these fuels build up with time, the likelihood of forest fires increases, providing ideal conditions for initiation (initial fire ignition) and propagation (fuels for subsequent fire stages) of fire (Alkhatib, 2013). Initial ignition is often triggered by hot, dry summer days with low humidity and high winds, which can quickly escalate into a widespread fire.

There are three types of forest fire: ground fire, surface fire, and crown fire. Ground fires occur below the forest floor in deep accumulation of peat, duff, humus and similar decomposed vegetation. The fires spreading on the ground are called surface fires. They can progress further by burning fire-intolerant understory vegetation (Alkhatib, 2013). A surface fire enters an uncontrollable stage as it starts to consume large boles of living or dead trees and spread into crowns, which is called crown fire. The primary energy source for crown fire is biomass (Agee and Skinner, 2005). The burning continues as long as favorable conditions persist, including factors like fuel availability, terrain, and challenging weather conditions such as elevated temperatures, high windspeed, and low humidity, which make it difficult to stop the fire. By the time a forest fire is noticed, a large forest area would have already burned down.

1.2 Environmental impact of forest fires

Anthropogenic climate change is expected to bring elevated temperatures from 1.4 to 6℃ by the end of the 21st century (IPCC 2001, 2003; Boulanger, Martinez and Segura, 2006), irregular precipitation patterns (Dore, 2005), increased wind speeds (Blennow *et al.* 2010), and severe and frequent droughts (Grillakis, 2019). The degradation of structural and compositional heterogeneity of forests contributes to higher tree mortality rates (fuel accumulation) and increased frequency and severity of forest fires (Knapp *et al.* 2017). About 1.76 billion tonnes of CO_2 were emitted alone by forest fires in 2021 (World Economic Forum, 2021). Forest fires emit other greenhouse gases such as methane (CH_4) and nitrous oxide (N_2O). These emissions highlight the significant environmental impact of forest fires.

1.3 Fire risk management

Integrating fire risk management is important for land-use planning and forest management strategies in fire-prone areas. Fire management practices involve manipulating fuel structures to decrease fuel density, implementing fuel breaks to obstruct fire spread, and managing fuel loads to reduce the likelihood of fire occurrence. According to Agee (1996), fuel structure management to minimize fuel load can be done manually (human labor to remove the fuels directly), mechanically (using machinery), or by prescribed burning. Prescribed burning is carried out in a controlled environment (such as moist conditions) and is beneficial in mitigating fire severity (Agee and Skinner, 2005) by removing fuels such as downed or dead trees. Fire management also includes integrating remote sensing technologies, which is helpful in early fire detection and subsequent monitoring (Jain *et al.* 2020; Kolden *et al.* 2012).

1.4 Remote sensing in fire mapping and forest structure analysis

Remote sensing is an efficient alternative to traditional in situ methods such as ground surveying, plot sampling, etc., which are time-consuming, labor-intensive, detailed, and cover smaller areas. Satellite data are inexpensive, cover large-scale areas, and possess traceable temporal and spatial changes that can extract information crucial for ecological studies and fire management.

Remote sensing entails acquiring information about various features on Earth's surface without any physical contact through detecting electromagnetic radiation by sensors mounted on different platforms such as aircraft, UAVs, and satellites. Spatial and temporal resolutions determine the utility of satellite images. Spatial

resolution is the pixel size represented by the earth's surface within a digital image, while temporal resolution is the image capture frequency. Higher spatial resolution generates detailed images, and higher temporal resolution indicates frequent monitoring (Hall, 2024).

The spectral resolution is the ability to distinguish between finer spectral bands/wavelengths of electromagnetic radiation. Specific spectral bands detect and analyze burned areas in fire mapping. Satellites such as Landsat series, MODIS (Moderate Resolution Imaging Spectroradiometer), and Sentinel-2 utilize combinations of red, green, blue, NIR (Near Infra-Red), SWIR (Short Wave Infra-Red) and TIR (Thermal Infra-Red). Sensitivity to soil moisture and vegetation health makes NIR and SWIR bands more important in detecting burned areas for fire mapping (Lechner, Foody, and Boyd, 2020; What are the best Landsat spectral bands for use in my research? | U.S. Geological Survey, 2024).

Fire severity mapping involves dNDVI (delta Normalized Vegetation Difference Vegetation Index) and dNBR (delta Normalized Burn Ratio). These indices measure the change in vegetation health and soil moisture before and after the fire event. dNDVI is calculated using NIR and red bands. dNDVI values vary from -1 to +1, where +1 indicates healthy vegetation, 0 indicates barren land or sparse vegetation, and -1 suggests the presence of water bodies. dNBR is calculated from NIR and SWIR and is sensitive to PAR (Photosynthetically Active Radiation), soil moisture reduction, and mineral soil (Key and Benson, 2006; Meddens, Kolden, and Lutz, 2016).

1.4.1 GEDI

The Global Ecosystem Dynamics Investigation (GEDI) mission by NASA, utilizing LiDAR (Light Detection and Ranging) technology, yields information about forest structure in burned areas. GEDI surpasses other missions because of its penetration capability of up to 99% in dense vegetation (Hoffrén et al., 2023). GEDI provides data on vertical canopy profiles for mapping continuous variables like canopy height, canopy cover, and aboveground biomass density in the survived forest patches because of the interaction in a vertical orientation (Myroniuk *et al.* 2023). GEDI data is inexpensive, freely available to the public, and has proven advantageous when the study location is inaccessible or field observation is not viable.

The GEDI-derived metrics are calibrated using field observation to ensure spatial accuracy. This process is also called co-registration. Various statistical regression models and machine learning algorithms are developed to understand and predict the relationship of GEDI metrics with field-observed metrics in the study location. After this, applying the prediction models to the GEDI data over the study location can generate maps for forest structures in larger areas. These maps are then utilized for fire impact assessment.

1.5 Chornobyl Exclusion Zone (ChEZ)

1.5.1 Chornobyl Exclusion Zone: past

Unlike any other forest fires, fire events in ChEZ have grave implications for future generations in the Northern Hemisphere. The nuclear explosion at the V.I. Lenin Power Plant in Chornobyl (Now known as the Chornobyl Nuclear Power Plant) on April 26th, 1986, contaminated (radionuclide contamination level> 37,000 Bq/m^2) more than 200,000 km^2 area of Europe majorly with ^{137}Cs ($T_{1/2}$ = 30.1 years), ^{90}Sr ($T_{1/2}$ = 29.14 years) and $^{238+239+240}Pu$ (Ager *et al.* 2019; Masson *et al.* 2021). During the following spring and summer in 1986, more than 300,000 people were evacuated by forming two exclusion zones around the Chornobyl Power Plant: Chornobyl Exclusion Zone (ChEZ; 260,000 ha) in Ukraine and Polesie State Radioecological Reserve (PER; 240,000 ha) in Belarus (Beresford *et al.* 2021). The radioactive fallout spread across the northern hemisphere, contaminating soil, forests, fields, and water bodies contingent upon wind and precipitation (Zhuravel, 2021). The forest cover of ChEZ was 41% in 1986 (Matsala *et al*. 2021a), which played a crucial role in containing these radionuclides and preventing further migrations through water or wind as dust and further propagation through trophic chains (Bird and Little, 2013). However, since then, smoke plumes of irradiated forest fires may redistribute some radionuclides to a greater distance within and outside ChEZ (Yoschenko *et al.* 2006), potentially polluting air, water bodies, and food.

1.5.2 Challenges in silviculture due to radioactivity

Silvicultural activities have been significantly hindered due to radioactivity. Before 1992, large-scale Scots pine plantations were established during the soviet era (Ager *et al.* 2019). Kashparov et al. (2024) reported that 80% of the forests in ChEZ are dominated by Scots pine (*Pinus sylvestris* L.), while silver birch (*Betula pendula*) and European oak (*Quercus robur*) cover 8-10% and 5-6% respectively in the present time. Local forest management activities are partially prohibited, and silvicultural interventions are mostly confined to making firebreaks or conducting intermediate thinning treatments (Zhuravel, 2021). Final felling and prescribed burning are completely prohibited.

As agricultural activities have also been banned since 1986, the farmlands were quickly afforested (Matsala *et al.* 2023). The partial prohibition of silvicultural treatments, such as pre-commercial thinnings, resulted in weak, flammable, overstocked Scots pine stands with reduced growth and high susceptibility to fire, pests, and diseases (Zymaroieva *et al.* 2023). Ager et al. (2019), Beresford et al. (2021), and Zymaroieva et al. (2023) suggest that the lack of silvicultural interventions and forest management have also led to the accumulation of fuels and

increased wildfire risk, which is further exacerbated by climate change. From 1993 to 2021, ChEZ experienced almost 1730 wildfires (*Zymaroieva et al.* 2023), out of which a few were mega-fires (1992, 2015-2016, 2020, and 2021). The last mega-fire incident in ChEZ happened in May 2022 during the Russian invasion.

Forestry activities are only carried out to ensure fire safety requirements by growing healthy, vital plantations for barrier function (Zhuravel, 2021). Deadwood removal or salvage logging is prohibited as the area is treated as a nature reserve (Matsala *et al.* 2023). Forest management and firefighting operations are hazardous and challenging, as radiation exposure poses significant health risks to workers and firefighters. Consequently, financial and logistical constraints, especially after the Russian invasion of Ukraine in 2022, further hinder effective forest management and fire control efforts in ChEZ.

1.6 Relevance of this study

In May 2022, a mega-fire in the southeastern part of the ChEZ triggered by the Russian invasion of Ukraine burned almost 14,000 ha of area (UNCG, 2023). This includes the forest plantations of different tree species established after the first ChEZ mega-fire in 1992 (Zibtsev *et al.*, 2015). However, several patches survived the fire in 2022. A detailed analysis of forest management data from 2016 shows that the survived forest patches were largely homogenous in species composition, comprised of broadleaved tree species with more than 80% of the canopy.

This finding suggests that the dominance of broadleaves could have significantly contributed to the survival of some forest patches during the mega-fire. Consequently, our research aims to identify the forest characteristics of their surroundings that could also increase their chance of escaping large, natural fires. We hypothesize that fuel discontinuity and structural heterogeneity in the adjacent neighborhood areas (buffers) affect the probability of a forest patch escaping fire.

The analytical approach involves a buffer-level spatial aggregation. In the first step, I calculated the mean values of canopy cover, canopy height, canopy height difference, and the presence of broadleaves within the buffers around the forest patches. Then, this aggregated data was fed to the classification models to predict whether each buffer was likely to be burned (non-refugia) or unburned (refugia). This approach is beneficial in understanding the factors in the surroundings that influenced the fire behavior, resulting in some patches being burned while others are not.

I used 10 m, 30 m, and 50 m buffers around the survived patches. I selected buffer widths of 10 m, 30 m, and 50 m to examine how the impact of surrounding patches varies with distance from the survived patches. We created external buffers

only because we expected them to be less homogeneous than the survived forest patches and differ mostly in forest structure.

Then, I collected variables representing vegetation in the buffers. This involved analyzing LiDAR data, forest management data, and satellite records. I used these variables to model the occurrence of refugia within these buffers.

I tested whether the hypotheses about fuel discontinuity and structural heterogeneity are true. Fuel discontinuity is the degree of interruption in continuous fuel distribution across the forest floor (Agee, 1993). Increased fuel discontinuity reduces fire spread. Canopy cover was the variable selected to examine fuel discontinuity because fire spread slows down when there is much variation in canopy cover, creating fuel breaks (Francis *et al.* 2023). As canopy cover decreases, fuel discontinuity increases due to vegetation gaps. Hence, more survived patches were expected under lower canopy cover values.

Structural heterogeneity is the variation in forest structures, such as differences in canopy heights and diameters. I chose canopy height difference to study structural heterogeneity because the presence of tall and short trees can interrupt fuel continuity, reducing the fire spread. More burned patches were anticipated for negative CH difference because short trees in the buffer may act as ladder fuels for crown fire in the main forest patches.

2. Materials and methods

2.1 Study area

Chornobyl Exclusion Zone (ChEZ) is a 2600 km^2 area formed after the nuclear explosion of 1986. ChEZ is located 100 Km north of Kyiv, in northern Ukraine, and borders Belarus (N 51.084 and N 51.351; E 29.262 and E 30.384). The area of interest possesses an Eastern European plain topography with a maximum elevation above sea level of 200m and is characterized by sod-podzolic soil. Pripyat River passes through, with swampy left banks and high right banks. The local climate is continental (for the last 66 years). The mean annual temperature is 8.20℃, and the mean annual precipitation is 620mm. As of 2020, the forest cover in ChEZ is 59% (Matsala *et al.* 2023), which was 41% in 1986. The region is a part of the Eastern European mixed forest belt, and the dominant local tree species include Scots pine (*Pinus sylvestris* L.), silver birch (*Betula pendula* Roth.), European oak (*Quercus robur* L.)., and common alder (*Alnus glutinosa* (Gaertn.) L.).

Many forest patches were established in our study area in the southeastern part of ChEZ after the first mega-fire in 1992. Some of these patches survived the last mega-fire in May 2022, forming the basis of our study (Figures *1*, *2*, and *3*).

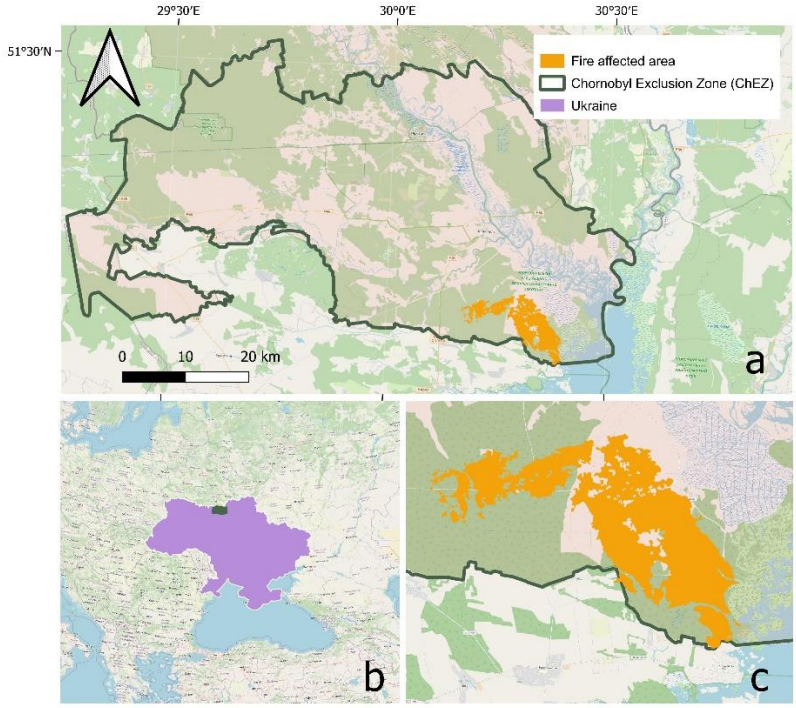

Figure.1: The maps of Ukraine and the area in ChEZ affected by the mega-fire in 2022.

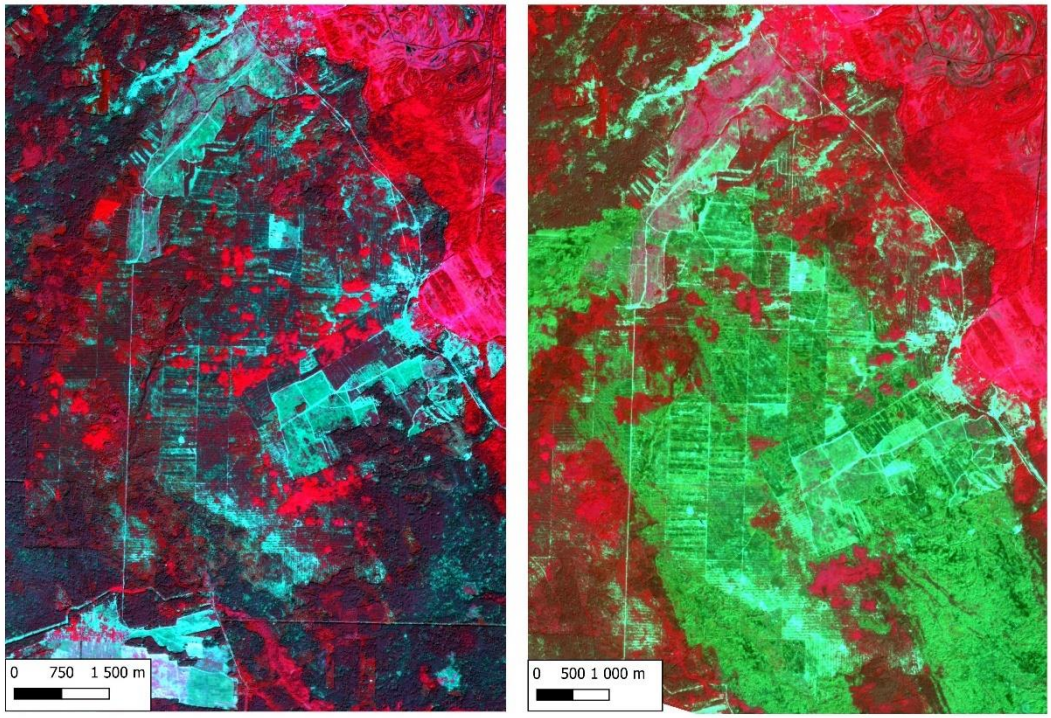

Figure 2: False color composite showing pre-fire (left) and post-fire (right) Planet satellite images of the study area. The red color indicates the presence of healthy vegetation, while the green color shows the area affected by the fire.

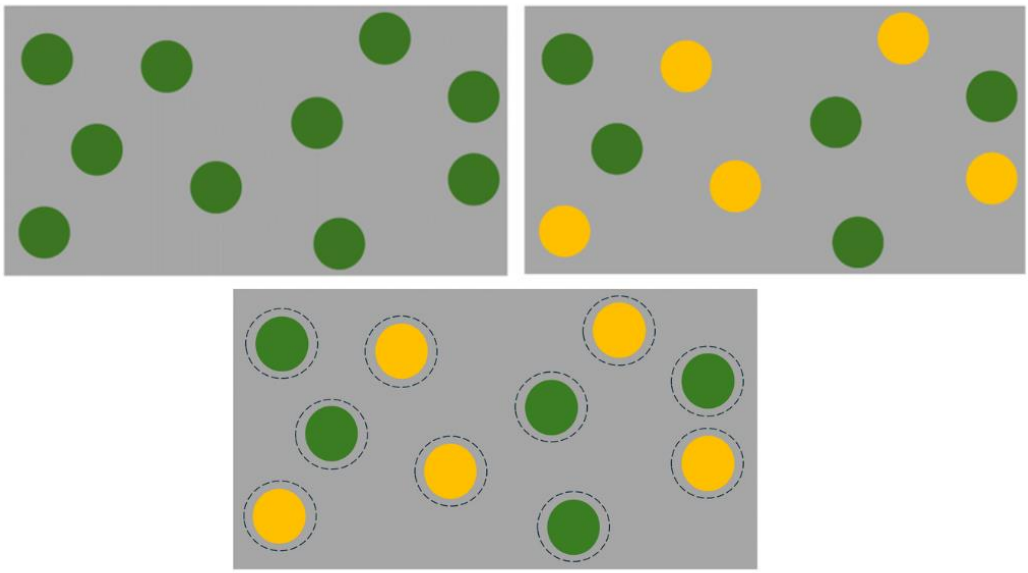

Figure 3: A schematic representation of the study area. Top left: The grey area denotes the fire-affected area from the 1992 mega-fire. The green circles show the broadleaved patches established following the fire. Top right: During the second mega-fire in May 2022, some patches burned (yellow), but others survived (green). Bottom: Our research aims to understand the factors in their buffers (dashed circles) influencing forest patches' fire behavior and survival.

From the forest management datasets of 2016, the main species prevailing in the area are Scots pine, silver birch, European/pedunculate oak(*Quercus robur*), European aspen(*Populus tremula*), and common alder(*Alnus glutinosa*). Other minor tree species include European hornbeam (*Carpinus betulus*), black locust (*Robinia pseudoacacia*), maple (*Acer* spp.), and Norway Spruce (*Picea abies*). The mean age of the stands is 58 years, with a maximum age reported 160 years and a minimum age of 5 years. The standard deviation in age was 26.26 years. The mean stand diameter at breast height (DBH) is 23.20 cm, with a maximum DBH of 64 cm and a standard deviation of 9.5 cm. The mean stand height is 19.28 m with a maximum of 35 m, a minimum of 1 m height, and a standard deviation of 6.53 m. The average growing stock volume (GSV) was reported to be 249.9433 $m^3 \cdot ha^{-1}$ with the highest GSV of 620 $m^3 \cdot ha^{-1}$, the lowest GSV of 5 $m^3 \cdot ha^{-1,}$ and a standard deviation of 128.81 $m^3 \cdot ha^{-1}$. There are some outliers for Scots pine in age, diameter, and GSV in the graph below (*Figure 4*). They are from the oldest Scots pine stands, established during the Soviet reign.

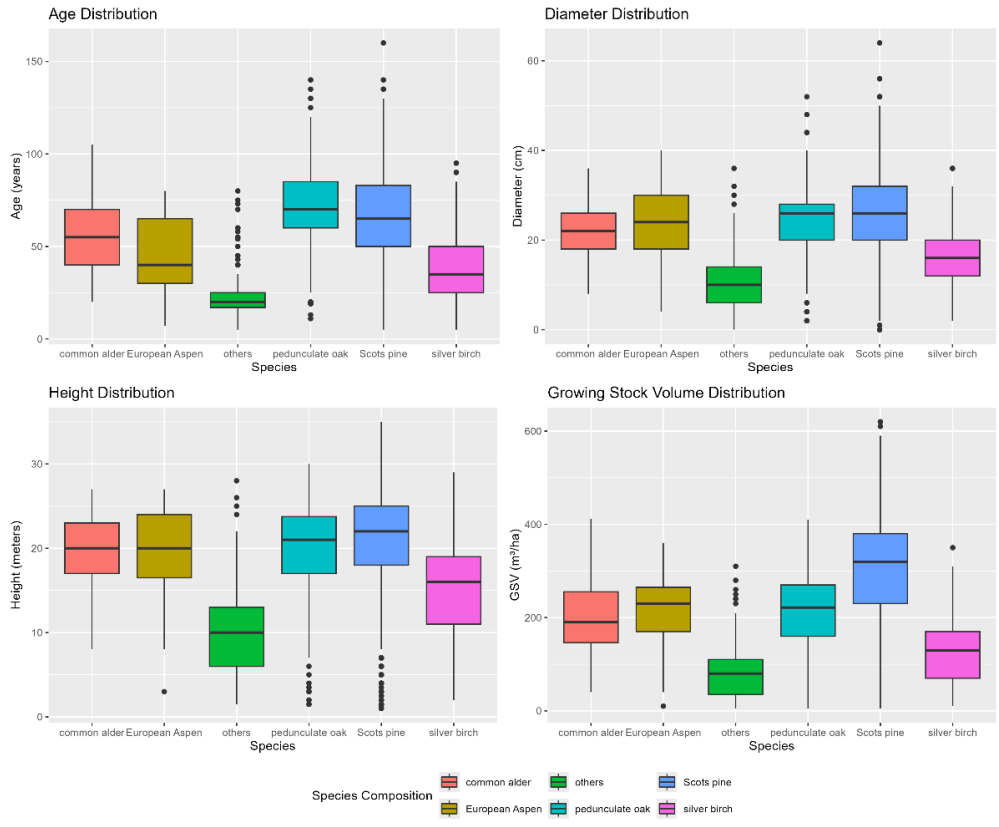

Figure 4: Distribution of age, mean stand DBH, growing stock volume (GSV), and mean height, respectively, from the forest management plan from 2016

2.2 Data

2.2.1 Shapefiles

The stand-wise forest management data was obtained in 2016 and was provided as a set of stand-level polygons. The polygons here contain data on variables such as stand tree species composition, mean height, DBH, GSV, and age.

2.2.2 GEDI

The GEDI LIDAR footprints for the study were downloaded from the Google Earth Engine (GEE) platform. GEDI is a LiDAR instrument mounted on ISS by NASA that provides high-resolution laser altimetry data, which contains detailed information on the vertical structures of forests (canopy cover and canopy height) and the terrain beneath. GEDI produces raw, high-resolution, three-dimensional point clouds and waveform data representing the vertical fuel distribution on the ground surface (Liu and Wang, 2022). It was obtained as raster files containing the data on the canopy cover (CC). The values of CC ranged from 0 to 1.0. Then, it was vectorized to extract the average spectral values within each polygon and to derive calibration data to create a wall-to-wall CC map.

2.2.3 Raster files

Raster files of Planet satellite images of the study location in ChEZ before (2021) and after the mega-fire in 2022 with a spatial resolution of 3 m and eight spectral resolution bands were provided. This study uses eight spectral bands: NIR, red-edge, red, green, green_i, yellow, blue, and coastal blue. The green_i band is an optimized version with improved calibration of the green band. We used Planet imagery to map forest structure and composition in a spatially explicit, wall-to-wall manner.

We also used an existing, unpublished canopy height raster predicted from GEDI footprints with the data at 98% of relative height within a single footprint and Planet spectral variables.

2.3 Methods

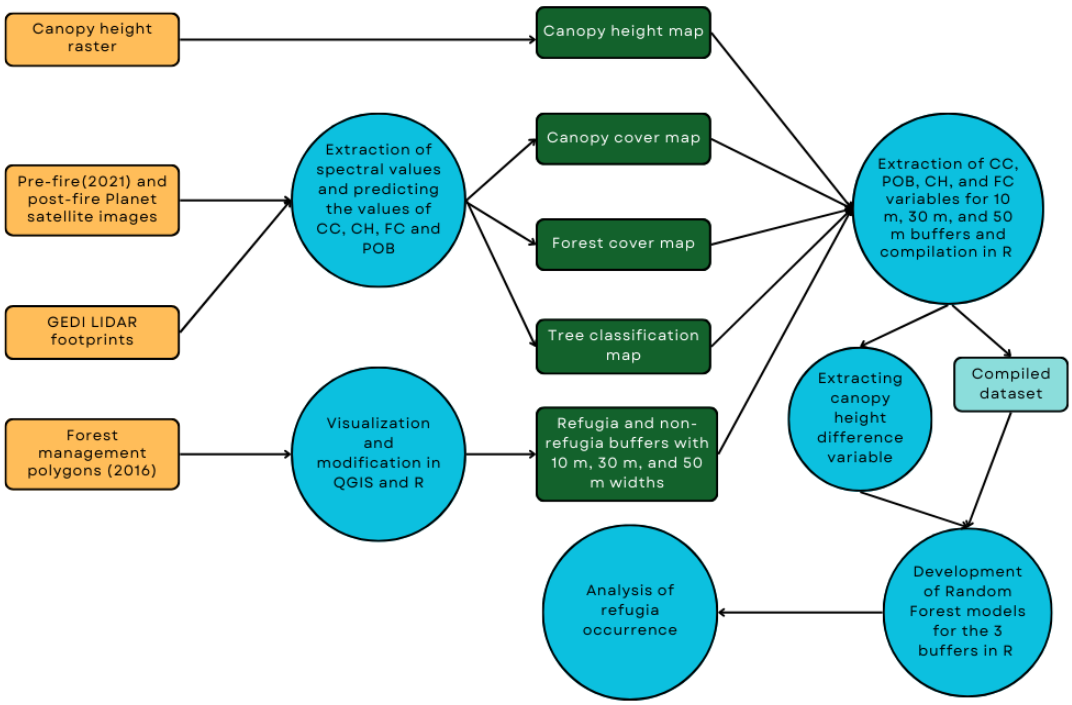

Figure 5: The workflow design for data processing and analysis

2.3.1 Modification of polygons

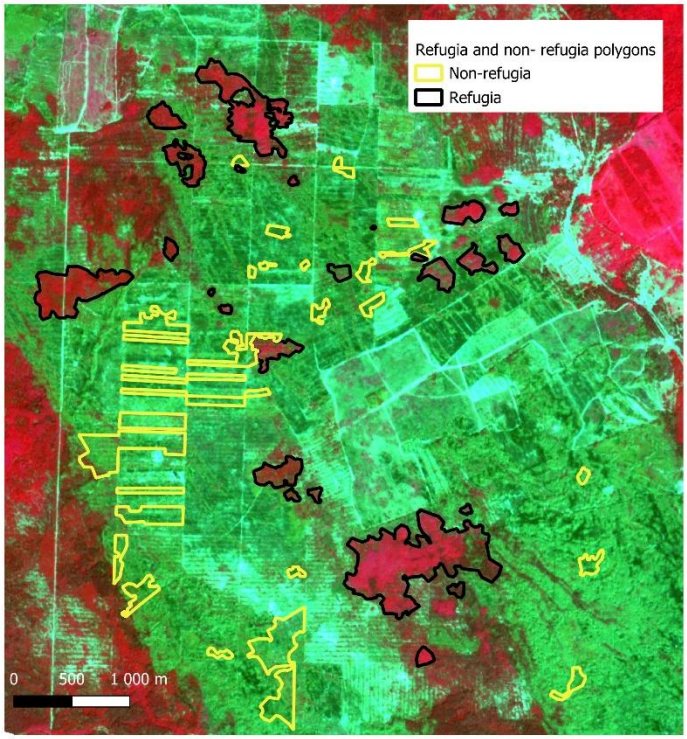

Figure 6: The refugia and non-refugia polygons created for the study. The post-fire Planet satellite image's false-color composite was used as a background image with a spectral band combination of near-infrared (NIR), red, and green.

The shapefiles containing forest stand polygons were visually examined and edited into two shapefiles to contain the fire refugia (survived forest patches) and non-refugia (burned forest patches). For visual examination, we used the post-fire Planet image's false color composite (NIR, red, and green). Only young broadleaved patches ≤ 38 years old (planted after the 1986 nuclear disaster) were selected to study the fire refugia occurrence. Quantum GIS (QGIS) Ver.3.28.0 (Firenze) was used to edit the shapefiles. Then, buffers of width 10 m, 30 m, and 50 m were created for both polygon layers (refugia set and non-refugia set) using R software. Buffers were created to identify the forest structure in the adjacent neighborhood areas of survived and burned patches. A total of 58 buffers were created, out of which 25 were non-refugia buffers, while 33 were refugia buffers. The refugia buffers were mapped only in the direction of fire blown by the wind. Figures *7(a)* and *7(b)* show refugia and non-refugia polygons for 10 m, 30 m, and 50 m buffers.

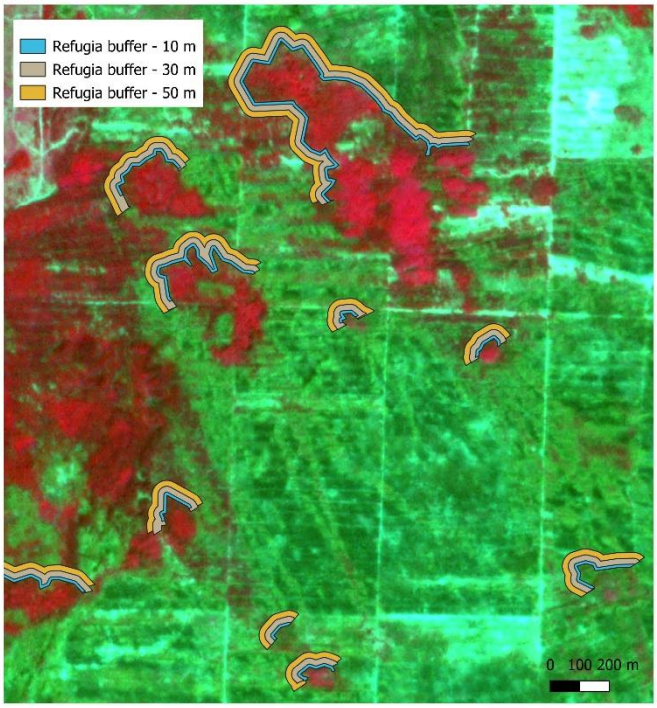

Figure 7(a). Visualization of refugia buffers with 10 m, 30 m, and 50 m widths.

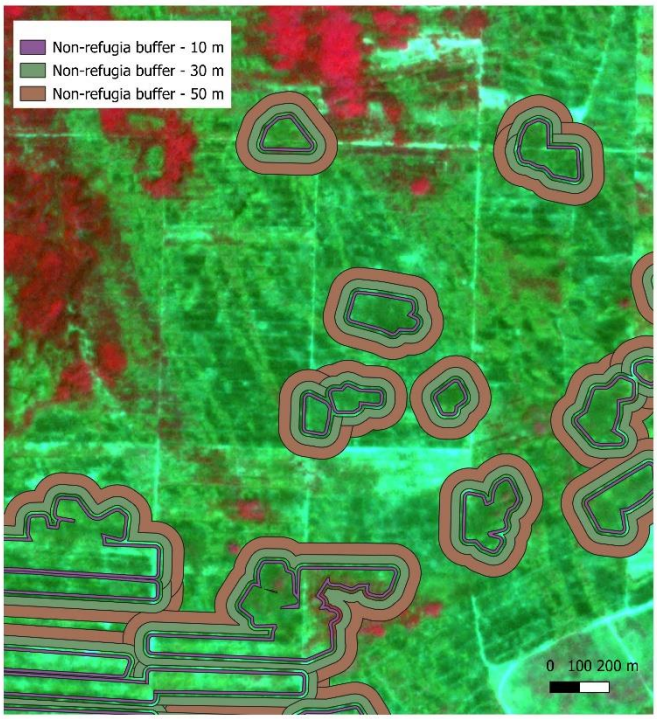

Figure 7(b). Visualization of non-refugia buffers with 10 m, 30 m, and 50 m widths.

2.3.2 Prediction models from remote sensing data

2.3.2.1 Random Forest

The Random Forest is a fast, accurate machine-learning algorithm (Breiman, 2001) used in classification and regression models. It works by building a "forest" of decision trees (for simple, non-parametric models), and each decision tree is trained by a random subset of the sample (training data) with random features. The only difference is that the target variables are class labels in classification, while in regression, they are continuous numerical values (Liaw and Wiener, 2022).

Even though GEDI provides high-resolution, precise data on canopy cover and canopy height, it is sparse and has limited coverage. To address this issue, we trained RF models using GEDI data with satellite imagery to predict canopy cover and canopy height across the entire study area. This approach enhances the predictive power of models beyond the limit of GEDI data points. Xi et al. (2022) demonstrated that RF prediction models are more suitable for extracting spatially continuous data for canopy height for the study area.

2.3.2.2 Forest cover model

The training dataset for the Forest Cover (FC) model was created using the pre-fire satellite image from 2021 with 3 m spatial resolution. Based on the visual interpretation as a true-colour image in QGIS, a shapefile (point vector) containing forest and non-forest points with binary values was manually created. The points that fall in areas with forest cover are assigned the value of 1, and those that fall in non-forest areas such as roads, agricultural fields, and grasslands were assigned the value of 0. The points were positioned at least 200 m apart to ensure statistical independence and avoid spatial autocorrelation.

R packages of `tidyverse, raster, terra, and randomForest` (Hesselbarth et al. 2021; Maxwell, Farhadpour, and Das, 2024) were used to develop the FC classification model using spectral Planet data as independent variables. After loading the satellite raster image from 2021 and point vector polygons in R, the mean spectral reflectance values for each point in the shapefile were extracted to create data frames. Then, a binary variable indicating forest presence was converted into a factor for facilitating classification (here, categorical mapping). A Random Forest model was trained to classify forest and non-forest areas using the extracted spectral values as the predictor variables. This mask was used to filter the study area only to the FC extent, thus masking out non-forest pixels. The FC model used all the spectral bands (coastal blue, blue, green, green_i, red, red-edge, yellow, and NIR) as predictor variables.

In the case of imbalanced data distribution (where one class is more prevalent than the other), the performance of classification models was assessed by classification accuracy metrics such as balanced accuracy, kappa, and F1 scores. The R package utilized for this operation was `caret` and the function `confusionMatrix()`.

2.3.2.2.1 Kappa coefficient

Cohen (1960) introduced the kappa coefficient as a statistical measure of overall agreement between categorical variables (Kvålseth, 1989). It can be used to understand how the model performs compared to random guessing. Kappa values range from -1 to +1. +1 indicates perfect agreement, 0 shows no agreement by chance, and -1 indicates less than an agreement by chance.

$$Kappa\ coefficient = \frac{P_0 - P_e}{1 - P_e}$$

Where,

P_0 = Observed agreement (Proportion of times the raters agree.)

P_e = Expected agreement (Proportion of times the raters are expected to agree by chance.)

2.3.2.2.2 F1 score

I used the F1 score to measure the model's accuracy on a dataset with an imbalanced class distribution. It is calculated as the harmonic mean of precision and recall (Lipton, Elkan and Narayanaswamy, 2014):

$$F1\ score = 2\ \times \left(\frac{Precision \times Recall}{Precision + Recall}\right)$$

Where,

Precision = Proportion of correct positive predictions

$$Precision = \frac{True\ positives}{True\ positives + False\ positives}$$

Recall for negative classes is known as specificity, and recall for positive classes is known as sensitivity.

Sensitivity = Proportion of actual positives correctly identified by the model.

$$Recall(Sensitivity) = \frac{True\ positives}{True\ positives + False\ negatives}$$

Specificity = Proportion of actual negatives correctly identified by the model.

$$Recall(Specificity) = \frac{True\ negatives}{True\ negatives + False\ positives}$$

2.3.2.2.3 Balanced accuracy

I calculated Balanced accuracy as the average of sensitivity and specificity:

$$Balanced\ accuracy = \frac{Sensitivity + Specificity}{2}$$

It is a robust measure that accounts for model performance on negative and positive classes and ensures better performance across all classes.

2.3.2.3 Canopy Cover Model

The canopy cover model was developed as a proxy for the hypothesis of fuel discontinuity. Because the fire spread is often limited under high variation in canopy cover (Francis *et al.,* 2023). The raster data with canopy cover from GEDI LiDAR footprints has been converted into a CC shapefile. R packages of `tidyverse`, `raster`, `terra`, and `randomForest` were used to develop the CC model. After loading the satellite image from 2021 and CC polygons into R, the Planet image was clipped and masked using the FC mask created earlier. This results in a forest mask raster, with non-forest areas (value 0) denoted as NA. The mean spectral reflectance values were extracted from the masked satellite image after assigning unique IDs to each polygon. NA values were filtered out, and I randomly sampled 1,000 polygons for training and 500 for validation.

The RF regression model of CC used yellow, red, red-edge, and NIR as predictor variables to predict the binary variable of Refugia and grew 500 decision trees. Other spectral bands, such as blue, green, and coastal blue, were not chosen as predictor variables since these increased the variation of the predicted CC in test model runs. The model performance was visually assessed by plotting predicted and observed values after making predictions on the validation set and finding root mean square error (RMSE). RMSE can be calculated using the rmse() function by loading `metrics` package in R or by the equation:

$$RMSE = \sqrt{MSE} = \sqrt{\frac{\sum_{i=1}^{n}(x_i - \bar{x})^2}{n-1}}$$

Where,

x_i = actual value
$\bar{x}$ = predicted value
n = number of data points

The model is then applied to the Planet raster image (masked within the forest cover map) for the wall-to-wall CC mapping.

2.3.2.4 Tree species classification model

A tree species classification model was developed to determine whether fuel type (coniferous and broadleaved) is involved in refugia occurrence. After visually examining the forest management stand polygons, a binary variable showing tree species composition has been created by selecting 100 coniferous and 100 broadleaved stands. Values of 0 were assigned to the stand dominated by any broadleaves (broadleaves proportion in growing stock volume should be ≥ 80%), and one was assigned to monocultures of conifers (pine proportion in growing stock volume should be ≥ 80%). Mixed stands with conifers and broadleaves were not selected. This was because mixed stands cause spectral mixing, which brings errors in the classification model. Stands with many open gaps in the canopy cover were also not selected, as they could also increase the model uncertainty.

R packages of `tidyverse`, `raster`, `terra`, and `randomForest` were used to develop the tree species classification model. The binary variable of tree species composition was then converted to a factor. An RF model was trained using the values of spectral bands blue, coastal blue, green, green_i, red, yellow, red-edge, and NIR as predictor variables. The same metrics that were utilized to assess the accuracy of the FC model have been used to evaluate the accuracy of the model. I developed a mask predicting the class labels of conifer and broadleaves (tree species classification mask) and a mask with the probability of broadleaves occurrence (tree species probability mask). Both masks were then masked by the forest cover mask. I used a probability map to proxy broadleaves' presence and expressed it as a percentage of broadleaved spectral signature within a given pixel.

2.3.2.5 Canopy height model

The supervisor provided the Canopy Height (CH) regression RF model after developing it from the 2021 GEDI LiDAR footprints. I chose the 98th percentile of Relative Height (RH98) as the GEDI metric. RH98 is the value below which 98% of all data points of Relative Height have fallen (Adrah *et al.*, 2021). The seven spectral bands, except coastal blue, served as predictor variables. With 500 decision trees, the explained variance was 59.97%.

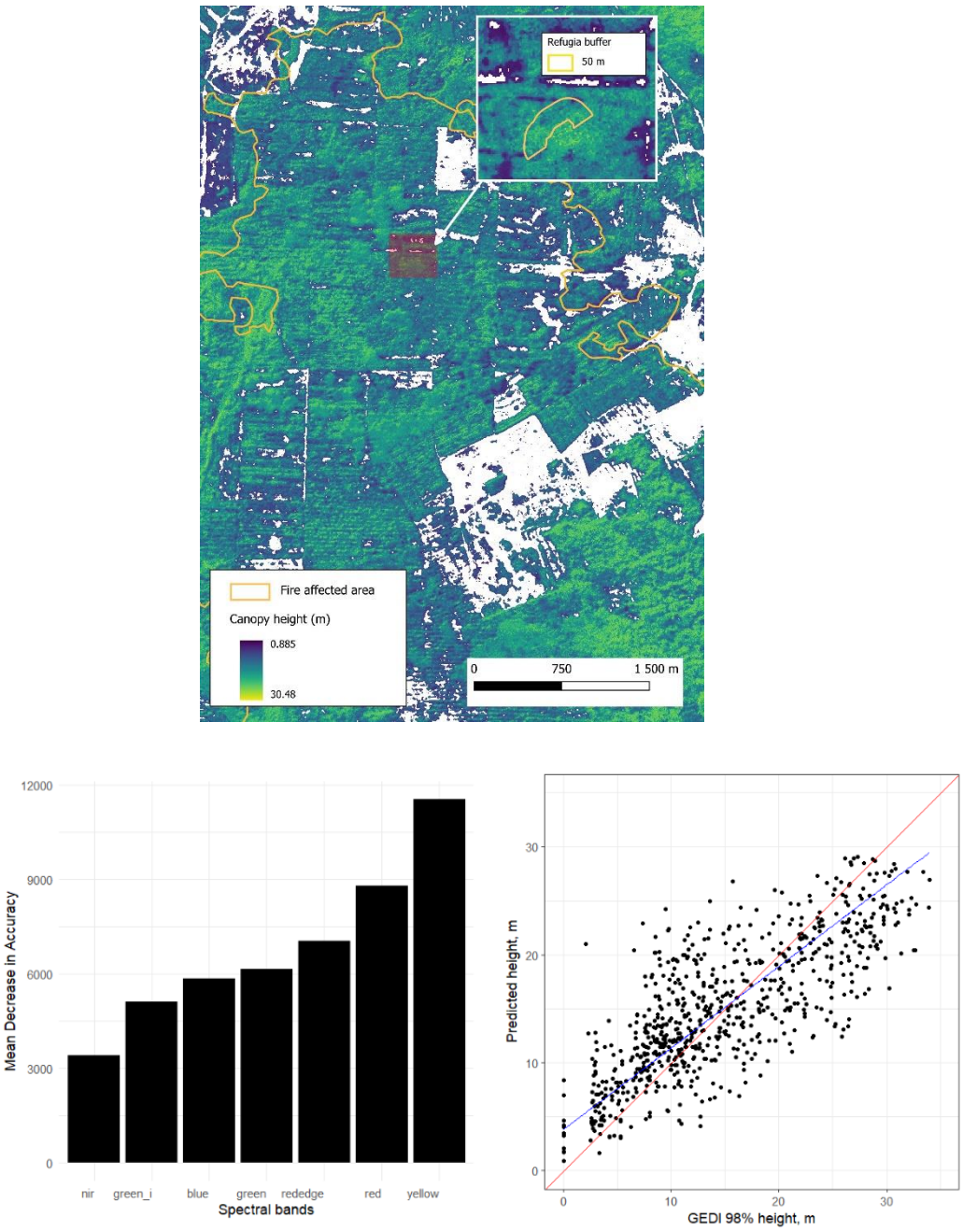

Figure 8: From top (a): The probability map for canopy height. The map shows the spatial distribution of canopy height over the study area. Bottom left(b): Variable importance plot for CH model. Only the yellow band significantly impacted the prediction accuracy of the CH model. Bottom right (c): Distribution of predicted and observed CH values. GEDI-based models underestimate higher CH values and overestimate lower CH values.

2.3.3 Extraction of data and analysis

The data fed into the models for classifying patches as either refugia or non-refugia based on the variables of canopy cover (CC), forest cover (FC), canopy height (CH), and broadleaves' presence (POB) as predictors. The choice of methods

(parametric or non-parametric) for further analysis was decided by testing the normality for the samples of each variable with the Shapiro-Wilk test.

The Shapiro-Wilk test is a statistical test used to assess whether a given sample came from a normally (Gaussian) distributed population. The null hypothesis, H_0, was that the population did not follow a normal distribution, while the alternative hypothesis, H_1, was that it did. A *p*-value less than 0.05 indicated that H_0 could be rejected and vice versa. The Shapiro-Wilk test for normality was performed on a random sample of 5,000 points after extracting canopy cover, forest cover, canopy height, and broadleaves' presence within the 10 m, 30 m, and 50 m buffers around refugia and non-refugia polygons. Most tests produced a p-value less than 0.05, indicating that the variable samples did not come from a normally distributed population at a 95% significance level. This finding (*Figure 9*) supported the choice of non-parametric data analysis methods, such as RandomForest (RF) modeling and General Additive Models (GAM). Penner, Pitt, and Woods (2013) demonstrated that RF offered operational advantages over parametric regression without compromising precision or accuracy.

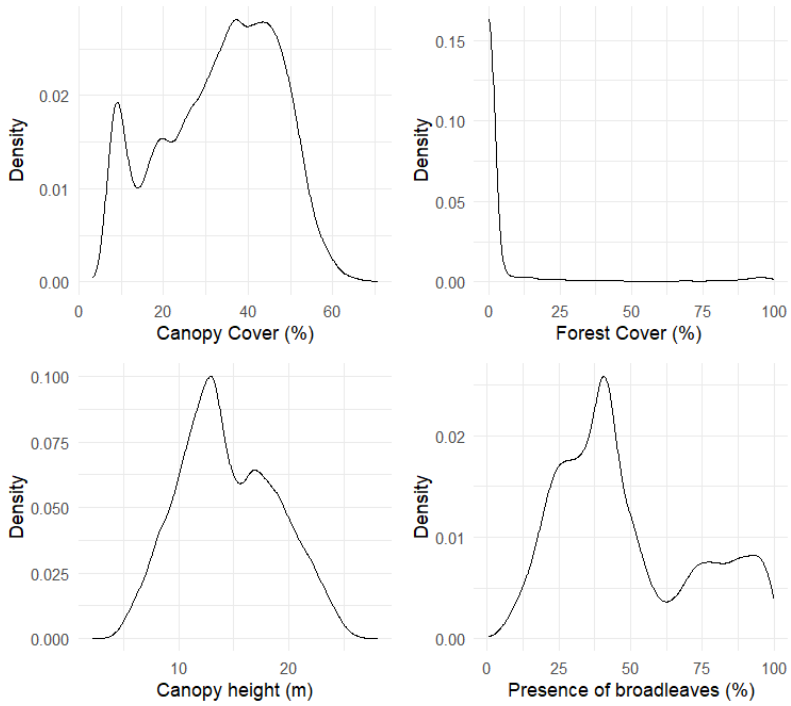

Figure 9. Distribution of sample values for canopy cover (CC), canopy height (CH), forest cover (FC), and presence of broadleaves (POB). All variables resulted in p-values <0.05. The Shapiro-Wilk test indicates that their distributions significantly deviated from normality at a 95% confidence level.

Then, I extracted the mean values of CC and CH for 10 m, 30 m, and 50 m buffers (refugia and non-refugia) and survived patch polygons into a large dataset.

I included another variable, CH-difference between each 10 m, 30 m, and 50 m buffer and the corresponding stand polygon, to check whether the hypothesis of structural heterogeneity was true. This dataset was the base for developing RF models for further analysis.

Three RF models were developed for every buffer width (10 m, 30 m, and 50 m) predicting the binary variable "refugia," which shows whether the target stand survived. R packages such as tidyverse, sf, terra, and randomForest were used for this purpose. The binary prediction variable refugia was converted into a factor by assigning 0 as burned and 1 as alive value. The predictor variables for refugia prediction were CC, CH, POB, and CH difference for each buffer. The Random Forest models were named rf.10, rf.30, and rf.50 for 10m, 30m, and 50m buffers, respectively.

We plotted variable importance plots and partial dependence plots to interpret the results of RF models. Using both metrics together gives a detailed interpretation of the models as variable importance plots point out which variables are crucial in predicting, while partial dependence plots identify the specific effects of these variables on the prediction. Variable importance helps determine the significance of each feature in predicting the target variable by calculating the importance score (Greenwell, Boemke, and Gray, 2020). Partial dependence is different from variable importance as partial dependence helps visualize the effect of one or two variables on the predicted outcome and how a change in these variables affects the predicted outcome (Friedman, 2001).

3. Results

3.1 Evaluation of models' performance

3.1.1 FC and POB models

After growing 500 decision trees, the FC model had an OOB (Out-Of-Bag) error (internal error caused by misclassification) of 2.47%. *Table 1* shows the confusion matrix, and *Figure 10* shows the variable importance plot for the FC model.

Table 1. Confusion Matrix for FC Classification Model.

	non-forest	forest	Classification error
non-forest	93	4	4.123
forest	8	381	2.056

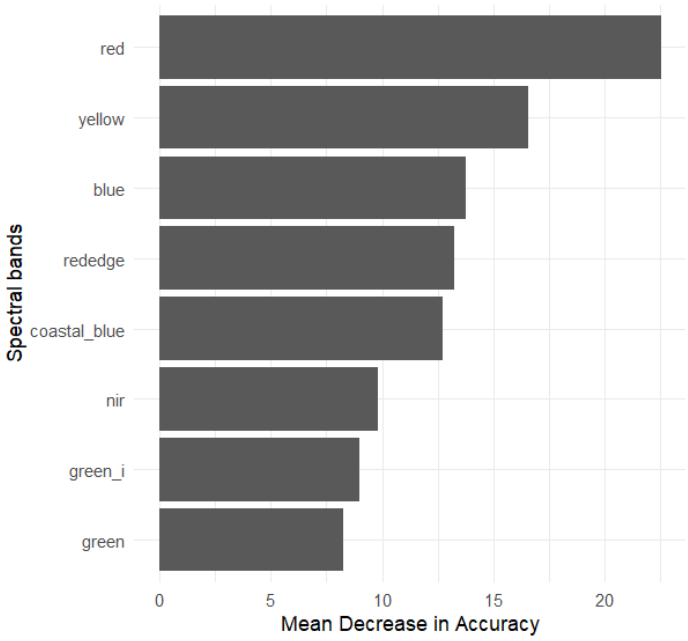

Figure 10. Variable importance plot for FC model.

After growing 500 decision trees, the OOB for the POB model was 16.92%. *Table 2* shows the confusion matrix, and *Figure 11* shows the variable Importance plot for the POB model.

Table 2. Confusion Matrix for POB Classification Model.

	coniferous	broadleaved	Classification error
coniferous	78	22	22.00
broadleaved	12	89	11.89

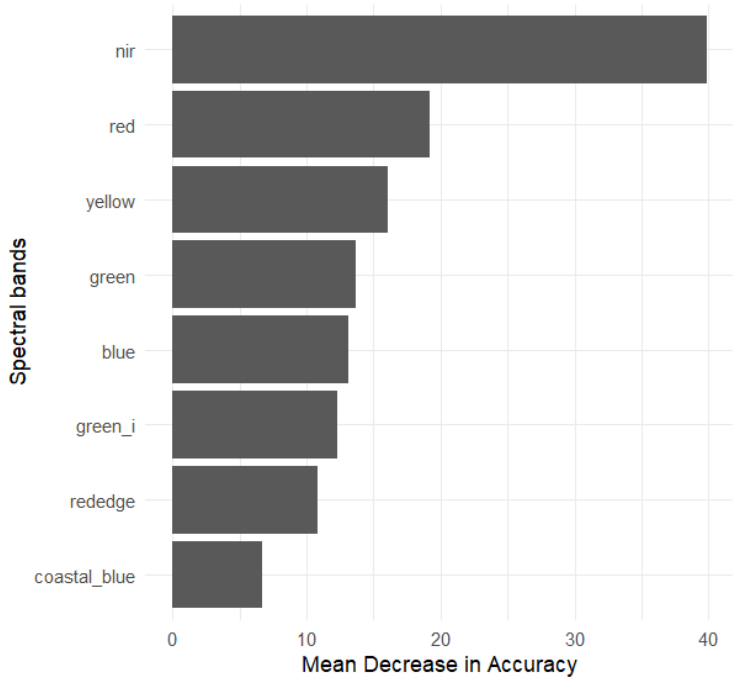

Figure 11. Variable importance plot for the POB model

Red and NIR bands significantly impact the accuracy of FC and POB models, respectively (*Figure 10* and *Figure 11*), suggesting that the red band was better at predicting FC and NIR was better at predicting POB.

Evaluation of POB and FC classification models yielded higher values of F1 score, kappa, and balanced accuracy (*Table 3*) for both of them but slightly higher for all three in the case of the FC model. Higher balanced accuracy (POB = 0.8506; FC = 0.9691) showed that the models performed excellently across both classes (forest and non-forest classes for FC; conifer and broadleaf classes for POB). Higher kappa coefficients (POB = 0.7014, FC = 0.9239) indicated that the models had better agreement with actual classes beyond what would be expected by chance. Higher F1 scores (POB = 0.8454; FC = 0.9394) indicated that the models accurately predicted positive classes.

Table 3. Model performance indicators for POB and FC models.

Model	Kappa	F1	Balanced accuracy
POB	0.6914	0.8394	0.8456
FC	0.9305	0.9447	0.9743

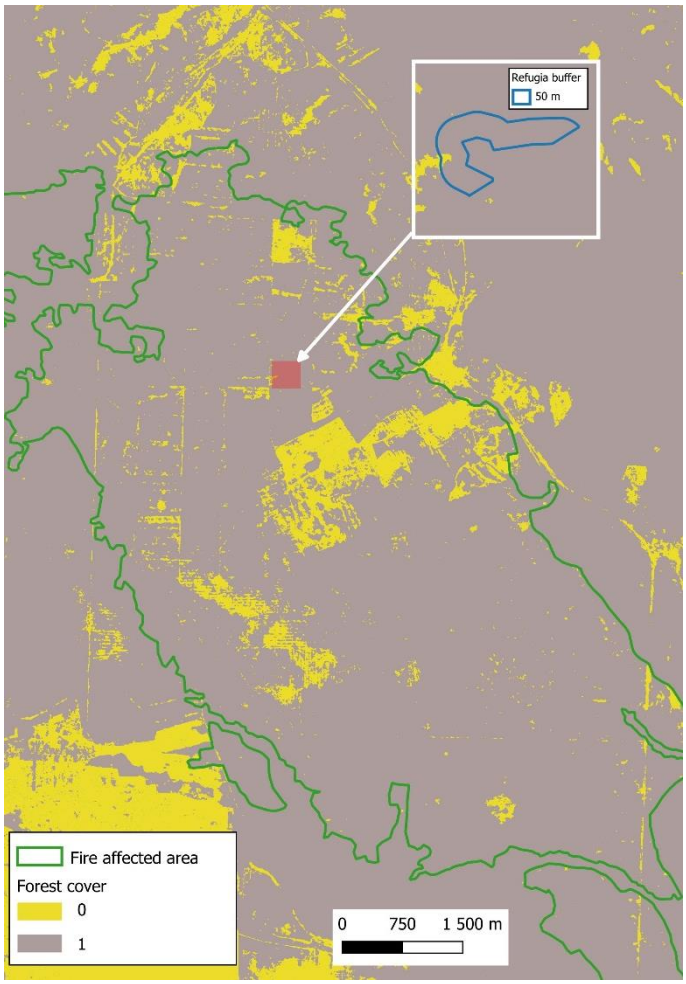

Figure 12: Probability map for forest cover for the study area. A value of 0 indicates a non-forest area, and 1 indicates that the area is a forest.

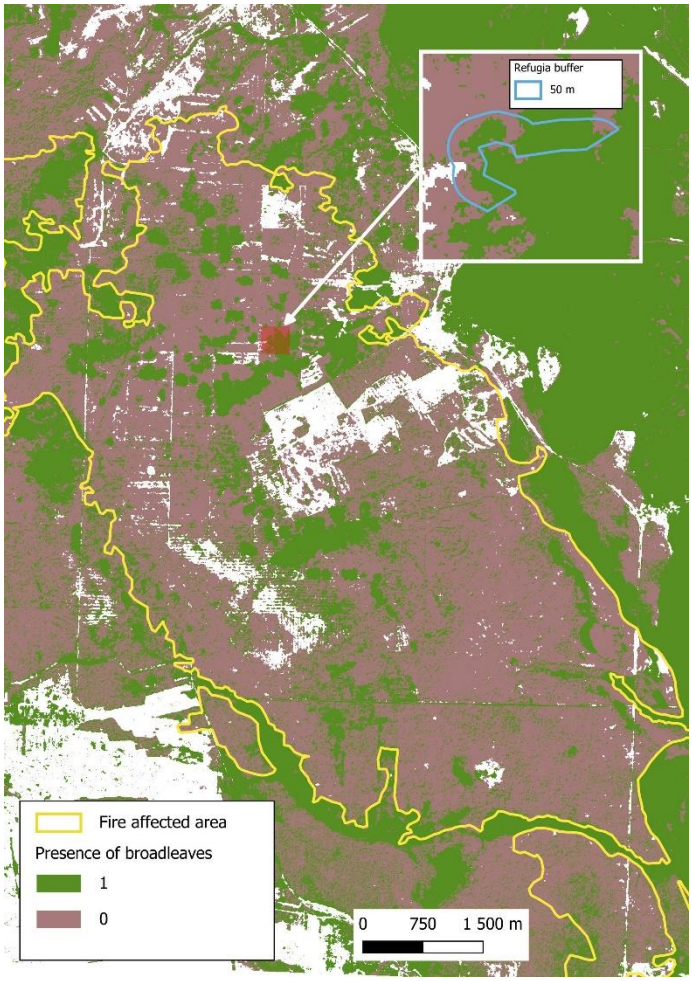

Figure 13: Probability map for the presence of broadleaves of the study area. A value of 1 indicates a higher presence of broadleaves, while 0 indicates a reduced presence.

3.1.2 Canopy cover model

The explained variance of this model was 23.31%, and the RMSE resulted in 0.1834. The mean value of CC was reported as 0.3680, and the relative RMSE was 49.84%. The red-edge band significantly impacted the accuracy of the CC model (*Figure 14(a)*).

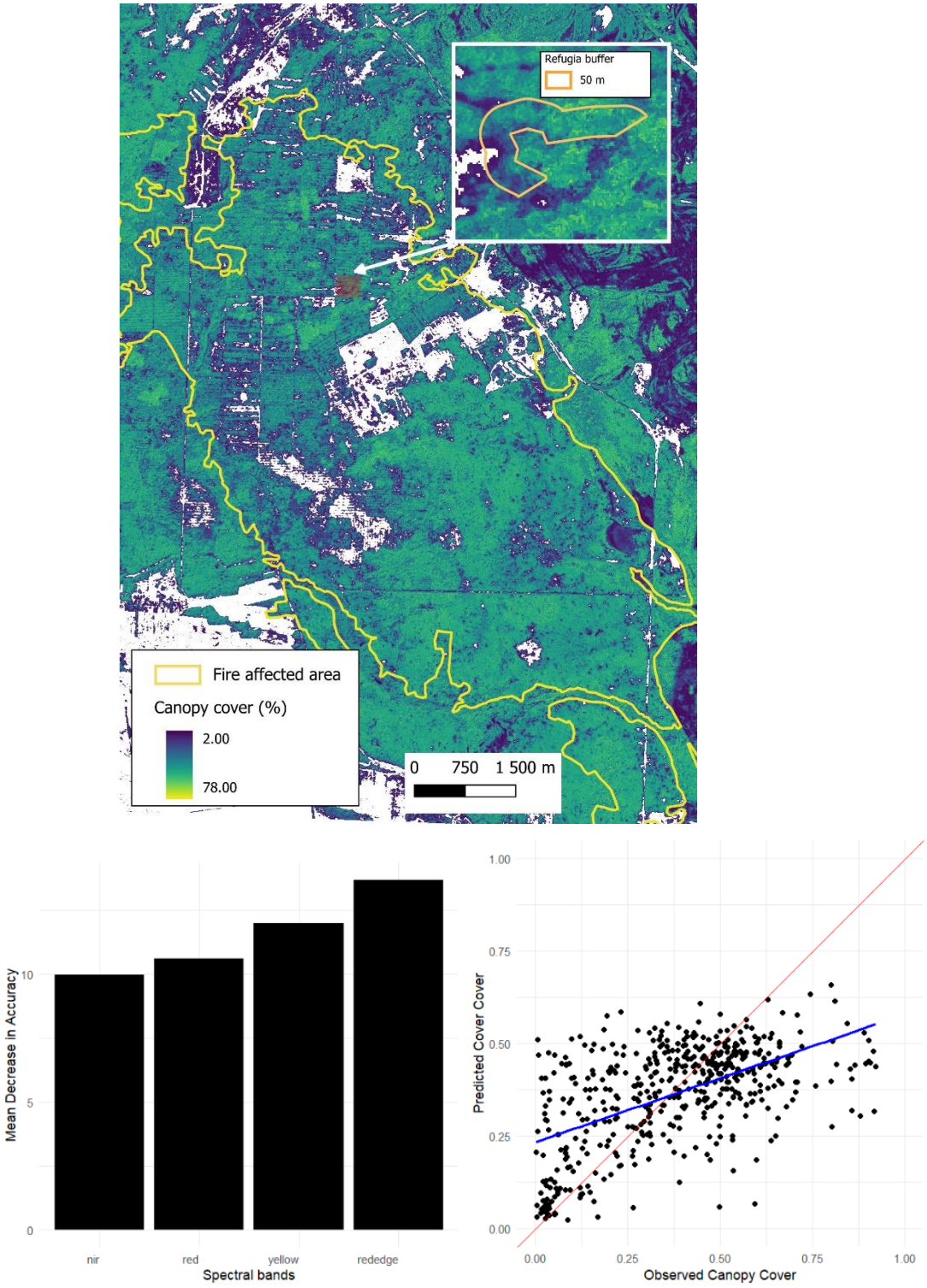

Figure 14. From top: (a) Probability map for canopy cover of the study area. Bottom left (b). The variable importance plot for the canopy cover model. Bottom right (c). Distribution of predicted and observed canopy cover values. GEDI-based models overestimate lower CC values while the higher CC values are underestimated.

3.2 Prediction models for buffers

3.2.1 Random Forest Models

The OOB error estimates for rf.10 was 31.03%, rf.30 was 25.86%, and rf.50 was 22.41%. Tables *4 (a),(b),* and *(c)* show the confusion matrix for each RF model. The classification error in the models was likely due to several reasons. One reason was the averaging of mixed conditions within buffer zones around each patch. As the vector layers cross the pixels of rasters, the buffer polygons could partially take the patches' values, leading to inaccuracies in the mean values of CH and CC. We did not attempt to create a raster mask of survived patches to exclude it from CC, CH, or POB rasters. Furthermore, the error could also be due to certain unaccounted factors, such as changing weather and topography.

Table 4(a). Confusion Matrix for rf.10.

	burned	alive	Classification error
burned	14	11	44.00
alive	7	26	21.21

Table 4(b). Confusion Matrix for rf.30

	burned	alive	Classification error
burned	15	10	40.00
alive	5	28	15.15

Table 4(c). Confusion Matrix for rf.50

	burned	alive	Classification error
burned	20	5	20.00
alive	8	25	24.24

3.2.2 Interpretation of Random Forest Prediction models' results

We developed variable importance plots and partial dependence plots to analyze the results of RF models.

3.2.2.1 Variable Importance Plots

Tables *5 (a),(b),* and *(c)* and Figures *15 (a),(b),* and *(c)* below show each RF model's importance scores of its predictor variables and variable importance plots, respectively. Variables with an importance score (MeanDecreaseAccuracy) ≤ 5.00 were not selected for further analysis as they did not yield useful information upon

further analysis. From the variable importance plots, we found that the variable POB has a higher importance score in all three Random Forest models for buffers with widths of 10m, 30m, and 50m (rf.10, rf.30, and rf.50, respectively), indicating that the POB has a significant impact on refugia occurrence in these buffers. Following POB, the CC variable possesses a moderate to low importance score for the RF models. Other variables, such as CH and CH difference, have lower importance scores, indicating no significant influence on predicting refugia occurrence.

rf.10:

Table 5(a). Importance score for rf.10

	alive	burned	MeanDecreaseAccuracy	MeanDecreaseGini
CC	1.13	11.23	9.167	7.113
POB	11.517	12.7	15.72	9.574
CH - difference	5.80	3.82	5.90	6.040

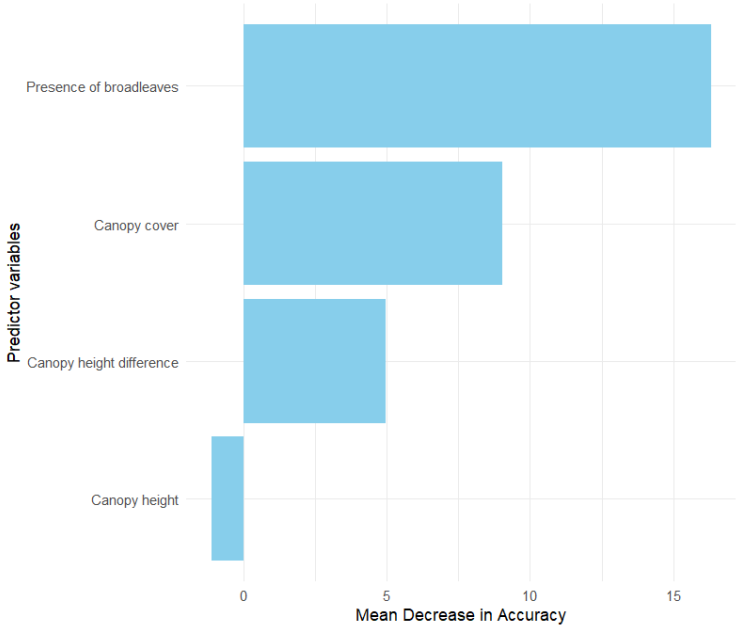

Figure 15(a). Variable importance plot for rf.10

rf.30:

Table 5(b). Importance score for rf.30

	alive	burned	MeanDecreaseAccuracy	MeanDecreaseGini
CC	0.4646	12.127	9.191	6.014
POB	20.655	22.94	26.64	12.69

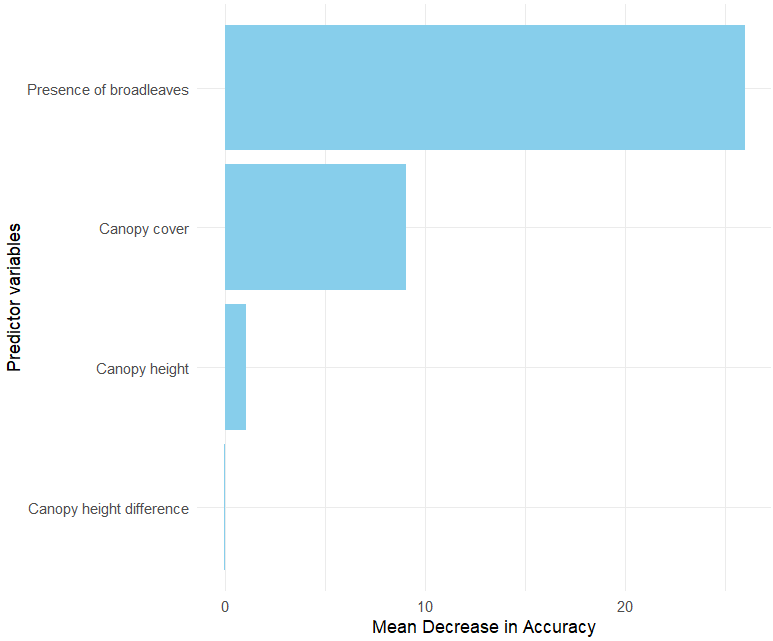

Figure 15(b). Variable importance plot for rf.30

rf.50:

Table 5(c). Importance score for rf.50

	alive	burned	MeanDecreaseAccuracy	MeanDecreaseGini
CC	2.659	14.02	12.89	6.00
POB	19.698	25.47	27.91	12.98

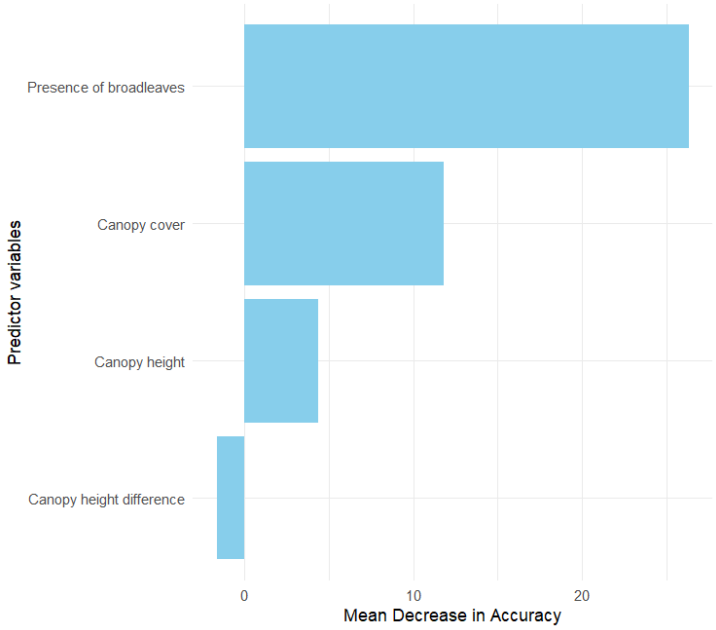

Figure 15(c). Variable Importance plot for rf.50

3.2.2.2 Partial Dependence Plots

Figures *16(a)*, *16(b)*, and *16(c)* are partial dependence plots for each predictor variable of rf.10, rf.30, and rf.50, respectively. The histograms represent the availability of data points of refugia polygons (sky blue) and non-refugia polygons (orange).

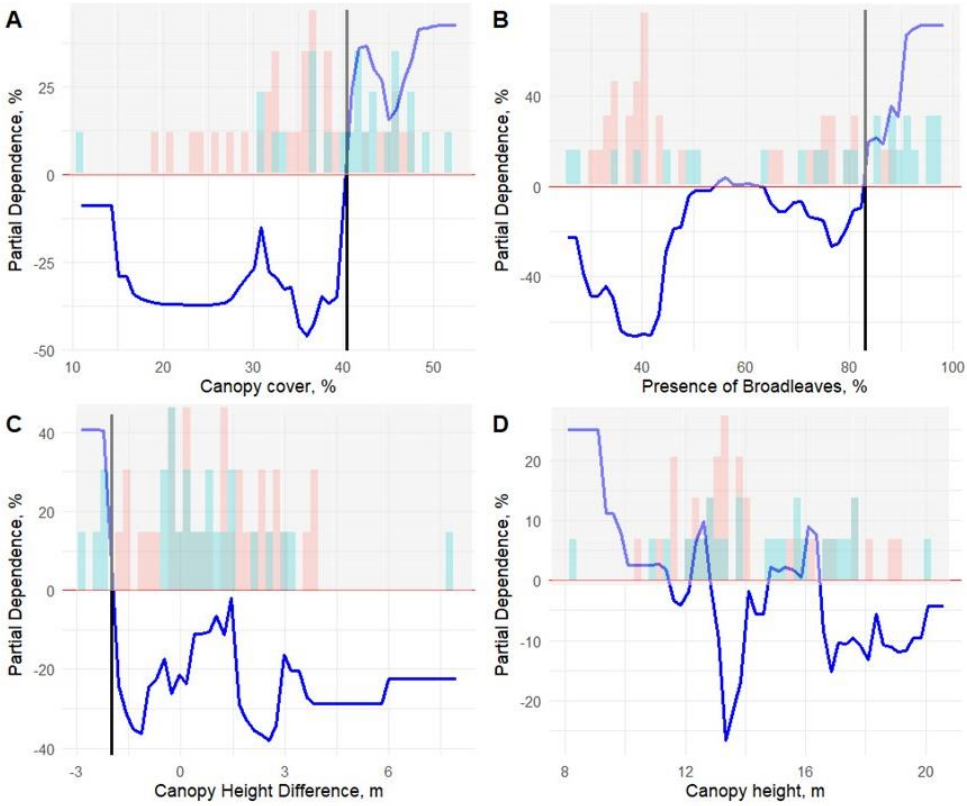

Figure 16(a). Partial dependence plots for variables CC, CH, CH-difference, and POB for rf.10.

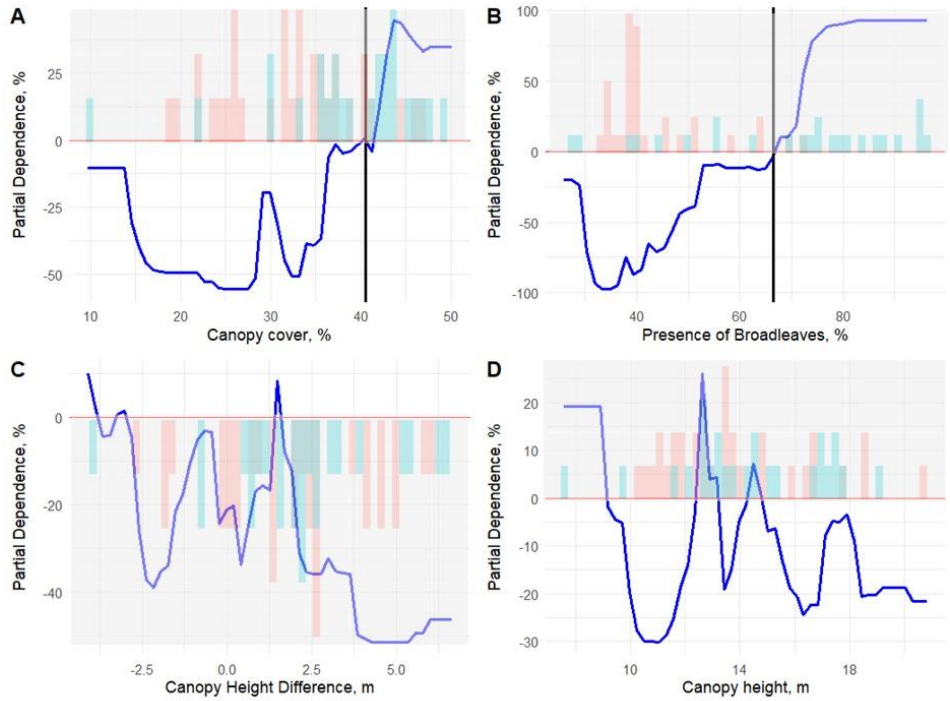

Figure 16(b). Partial dependence plots for variables CC, CH, CH-difference, and POB for rf.30.

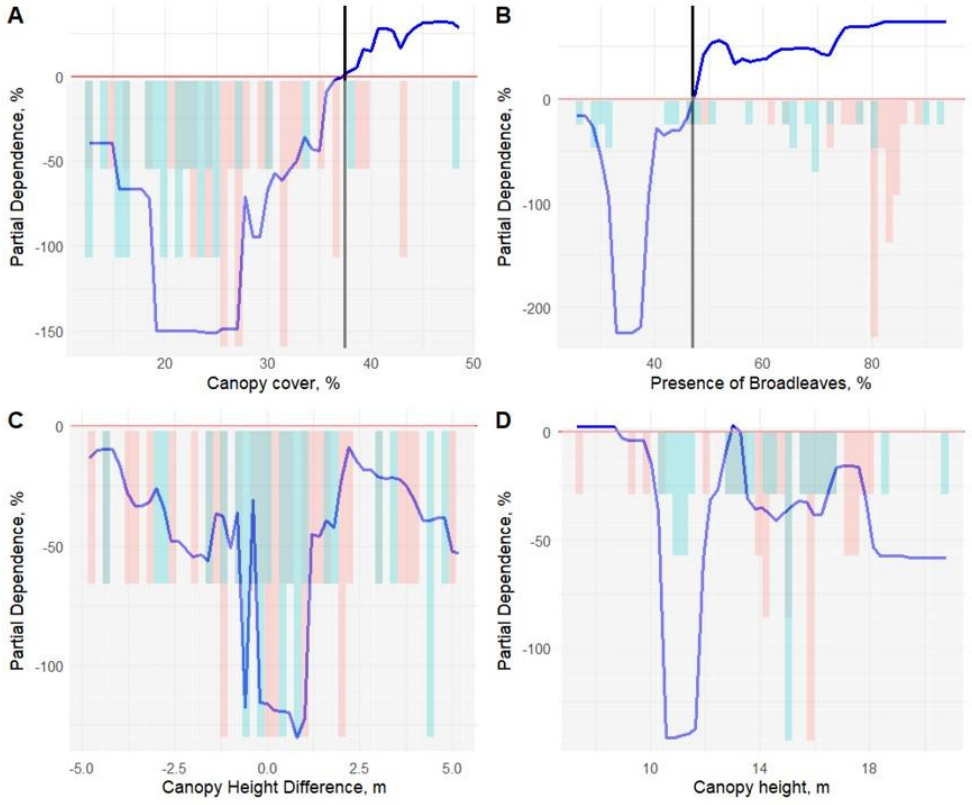

Figure 16(c). Partial dependence plots for variables CC, CH, CH-difference, and POB for rf.50.

The partial dependence plots indicate a positive trend for CC and POB in the RF models. The critical threshold values (the predictive outcome was negatively influenced below these values and positively above the values) observed for CC were 40.5%, 41.10%, and 37.5% for rf.10, rf.30, and rf.50, respectively.

The partial dependence plots for CH show a complex, non-linear relationship, while the CH difference for rf.10 has a critical threshold value of -2.26 m. A negative Canopy height difference means trees in the buffer are taller than those in survived patches. The canopy height difference continues to impact the refugia occurrence positively if the trees in the buffer are taller (2.26 m or more) than the trees in the polygon. However, this feature was observed only until the height difference of -2.26 m, after which it did not influence the prediction of refugia occurrence. For rf.30 and rf.50, we did not observe a critical threshold value.

The critical threshold values observed for POB in rf.10, rf.30, and rf.50 were 83%, 66%, and 47% respectively. A decline in partial dependence for rf.10 was observed between the POB values of 60-80% (*Figure 16(a)*). As for rf.30, there was a decline in partial dependence between POB values of 19-31 %, and POB has no significant influence over refugia occurrence after a slight increase after the critical threshold value (66%), as shown by the flat lines in the graph of POB in *Figure 16(b)*. Also, POB has no significant influence over refugia occurrence in rf.50.

4. Discussion

4.1 Influence of broadleaves in refugia occurrence

Our analysis did not provide evidence supporting hypotheses of fuel discontinuity and structural heterogeneity. The presence of broadleaves increased the probability of refugia occurrence; in contrast, canopy height in the buffer and canopy height difference (between the stand and its buffer) did not significantly impact refugia occurrence. Despite a higher importance score, the fuel discontinuity hypothesis was rejected because we observed more burned patches associated with lower canopy cover values (20-30%) for 10 m and 30 m buffers (*Figure 15(a)*), which was the opposite of what we anticipated. The structural heterogeneity hypothesis was rejected because we observed more refugia patches under negative canopy height difference, which was also the opposite of what we anticipated. There was a spike in data points for refugia areas below -2.26 m of canopy height difference, which caused an increase in the probability of refugia occurrence for rf.10. This created a critical threshold value of -2.26 m in rf.10. In contrast, the absence of critical threshold values for rf.30 and rf.50 may imply that structural heterogeneity could not save the forests from the mega-fire.

The observed decline in the probability of refugia occurrence for presence of broadleaves values between 60-75% and 19-36% in both rf.10 (*Figure 16(a)*) and rf.30 (*Figure 16(b)*) was because of limited data points available for refugia areas and a spike in data points for non-refugia areas, respectively. Additionally, the decrease in the probability of refugia occurrence for presence of broadleaves values of 60-79% can be attributed to the proximity of non-refugia buffers to highly flammable Scots pine stands. These stands burned, and the crown fire spread to surrounding patches, burning them down even when the presence of broadleaves values ranged between 75-81.5% in their 10m wide buffers. This effect also caused a decline in refugia occurrence in our models. The limited data availability and proximity to Scots pine stands have also affected the prediction of refugia occurrence in 30 m buffers.

4.2 Management implications

We recommend increasing the proportion of broadleaved species in production forests to reduce fire risk. Broadleaved species have higher foliage and wood moisture levels than conifers, reducing flammability and fire spread (Vallejo,

Arianoutsou, and Moreira, 2012). They can reduce vertical fire spread and crown fire risk as they act as ladder fuel breaks. The dense broadleaved stands are less affected by wind and cast intense shade with lower temperature and relative humidity due to decreased evaporation, which reduces fire risk (Whelan, 1995). Their leaves are quickly mineralized, preventing fuel accumulation on the forest floor and subsequent horizontal fire spread. Incorporating broadleaved species into local forest management plans can help develop resilient landscapes (Proença, Pereira, and Vicente, 2010; Pausas *et al.* 2005). Feurdean et al. (2017) also recommended increasing broadleaf deciduous forest cover in higher latitudes for fire suppression.

However, this study also observed that the efficiency of broadleaves in fire management depends on the landscape and the surrounding tree species. While they can act as a buffer, their effectiveness is compromised when adjacent to highly flammable species such as Scots pine, an excellent ladder fuel that can facilitate crown fire spread into the broadleaved stands. This means incorporating fire management strategies, such as implementing fuel breaks and removing fuel load, into the forest management regime could also enhance the resilience of broadleaved forests. Silvicultural activities such as thinning and prescribed burning are also essential in managing the fuel loads. Thinning from below in forest stands removes fine-diameter fuel load and reduces competition between trees for light, water, space, and nutrients. Reduction in competition leads to better resource allocation and growth rates and the development of thicker, fire-resistant barks for remaining trees (Moreau *et al.* 2022).

The high-density pine plantations (10,000 seedlings per hectare) in ChEZ witnessed dieback events due to droughts, accumulating fine-diameter fuels (Matsala *et al.* 2024). Pine forests exhibit a high load of dry, small fuels. Also, suspended needles and lower dead branches can act as ladder fuels (Proença, Pereira, and Vicente, 2010). This can facilitate crown fire spread in pine stands. Crown fire in Scots pine stands can then spread into adjacent broadleaved stands. Tree species such as black locust and European oak can sustain fire because of their thick bark and high moisture content. Despite higher fire resistance, black locust is an alien and invasive species in Europe as they propagate fast and outcompete native forest ecosystems. Once established, controlling and managing them becomes physically and economically exhausting. Hornbeam has thin bark and leaves with low moisture levels, while silver birch has thin bark and flammable leaves (USDA Forest Service, n.d.).

Fuel accumulation and lack of forest management promote fire spread in the study area. Ager et al. 2019 recommended developing strategies for harvesting deadwood contaminated by the deposition of nuclear fallout and managing it to facilitate further disintegration processes. Pre-commercial thinning of Scots pine plantations is also advisable as they are beneficial in removing ladder fuels. Also, a gradual

thinning is recommended because the dense forests in ChEZ provide an uninterrupted canopy for fire spread (Matsala *et al.* 2024). However, while pre-commercial and intermediate thinnings are partially prohibited in ChEZ, other silvicultural activities such as final felling, deadwood removal, and prescribed burning are completely prohibited (Matsala *et al*. 2021; Zhuravel, 2021).

4.3 Study limitations

Models based on GEDI spaceborne laser scanning data often generate biased estimates because the system cannot distinguish between grasslands and tree patches with heights less than 5m. As a result, similar values are assigned to both vegetation types. The underestimation of higher values and overestimation of lower values while predicting canopy cover (*Figure 13(b)*) and canopy height (*Figure 7(c)*) is another issue of concern. The underestimation of actual forest variable values occurred due to the ineffective laser penetration in denser canopies and reflecting the canopy surface only (Li *et al.* (2024); Liang *et al.* (2023)). The discrepancies in canopy cover estimates happen due to the averaging effects associated with the size of the laser footprint, which covers both forest and non-forest areas. As for canopy height, it happens when dense crowns obstruct the ground, leading to inaccurate estimates of actual canopy height.

Conclusions

Our study indicates that the forests that survived the May 2022 mega-fire in ChEZ were primarily due to the higher presence of broadleaved species in their surroundings. However, our findings did not support our hypothesis that structural heterogeneity and fuel discontinuity played a defining role. Broadleaved tree species such as European oak, European aspen, and silver birch can be introduced to create more mixed stands, as they are fire-resistant and ecologically resilient, thus facilitating post-fire ecosystem recovery. In addition to promoting broadleaves, it is also recommended that the proximity of any tree vegetation to conifer stands in fire-prone forests could be reduced to minimize crown fire risk in fire-prone forests.

References

Agee, J.K., 1996, January. The influence of forest structure on fire behavior. In Proceedings of the 17th annual forest vegetation management conference (pp. 52-68).

Agee, J.K. and Skinner, C.N., 2005. Basic principles of forest fuel reduction treatments. *Forest ecology and management*, *211*(1-2), pp.83-96.

Ager, A.A., Lasko, R., Myroniuk, V., Zibtsev, S., Day, M.A., Usenia, U., Bogomolov, V., Kovalets, I. and Evers, C.R., 2019. The wildfire problem in areas contaminated by the Chernobyl disaster. Science of the Total Environment, 696, p.133954. https://doi.org/10.1016/j.scitotenv.2019.133954.

Alkhatib, A.A. (2014) 'A review on forest fire detection techniques,' International Journal of Distributed Sensor Networks, 10(3), p. 597368. https://doi.org/10.1155/2014/597368.

Beresford, N.A., Barnett, C.L., Gashchak, S., Kashparov, V., Kirieiev, S.I., Levchuk, S., Morozova, V., Smith, J.T. and Wood, M.D., 2021. Wildfires in the Chornobyl exclusion zone—Risks and consequences. Integrated environmental assessment and management, 17(6), pp.1141-1150. https://doi.org/10.1002/ieam.4424.

Bird, W.A. and Little, J.B., 2013. A tale of two forests: addressing postnuclear radiation at Chernobyl and Fukushima. https://doi.org/10.1289/ehp.121-a78.

Blennow, K., Andersson, M., Sallnäs, O. and Olofsson, E., 2010. Climate change and the probability of wind damage in two Swedish forests. Forest Ecology and Management, 259(4), pp.818-830. https://doi.org/10.1016/j.foreco.2009.07.004.

Boulanger, J.P., Martinez, F. and Segura, E.C., 2006. Projection of future climate change conditions using IPCC simulations, neural networks and Bayesian statistics. Part 1: Temperature mean state and seasonal cycle in South America. Climate Dynamics, 27, pp.233-259. https://doi.org/10.1007/s00382-006-0134-8

Bowman, D.M., Balch, J.K., Artaxo, P., Bond, W.J., Carlson, J.M., Cochrane, M.A., d'Antonio, C.M., DeFries, R.S., Doyle, J.C., Harrison, S.P. and Johnston, F.H., 2009. Fire in the Earth system. *science*, *324*(5926), pp.481-484. https://doi.org/10.1126/science.1163886.

Bradstock, R.A., Hammill, K.A., Collins, L. and Price, O., 2010. Effects of weather, fuel and terrain on fire severity in topographically diverse landscapes of south-eastern Australia. Landscape Ecology, 25, pp.607-619. https://doi.org/10.1007/s10980-009-9443-8

Collins, L., Bennett, A.F., Leonard, S.W. and Penman, T.D., 2019. Wildfire refugia in forests: Severe fire weather and drought mute the influence of topography and

fuel age. *Global Change Biology*, *25*(11), pp.3829 3843. https://doi.org/10.1111/gcb.14735

Dore, M.H. (2005) 'Climate change and changes in global precipitation patterns: What do we know?,' Environment International, 31(8), pp. 1167–1181. https://doi.org/10.1016/j.envint.2005.03.004.

Feurdean, A., Veski, S., Florescu, G., Vannière, B., Pfeiffer, M., O'Hara, R.B., Stivrins, N., Amon, L., Heinsalu, A., Vassiljev, J. and Hickler, T., 2017. Broadleaf deciduous forest counterbalanced the direct effect of climate on Holocene fire regime in hemiboreal/boreal region (NE Europe). *Quaternary Science Reviews*, *169*, pp.378-390. https://doi.org/10.1016/j.quascirev.2017.05.024

Flannigan, M.D., Stocks, B.J. and Wotton, B.M. (2000) 'Climate change and forest fires,' *Science of the Total Environment*, 262(3), pp. 221–229. https://doi.org/10.1016/s0048-9697(00)00524-6.

Francis, E.J., Pourmohammadi, P., Steel, Z.L. *et al.* Proportion of forest area burned at high-severity increases with increasing forest cover and connectivity in western US watersheds. *Landsc Ecol* **38**, 2501–2518 (2023). https://doi.org/10.1007/s10980-023-01710-1

Grillakis, M. (2019) 'Increase in severe and extreme soil moisture droughts for Europe under climate change,' Science of the Total Environment, 660, pp. 1245–1255. https://doi.org/10.1016/j.scitotenv.2019.01.001.

Hall, C. (2024) What is Remote Sensing? https://www.earthdata.nasa.gov/learn/backgrounders/remote-sensing#:~:text=Resolution%20plays%20a%20role%20in,spatial%2C%20spectral%2C%20and%20temporal. (accessed on April 2nd, 2024)

Hesselbarth, M.H., Nowosad, J., Signer, J. and Graham, L.J., 2021. Open-source tools in R for landscape ecology. *Current Landscape Ecology Reports*, *6*(3), pp.97-111. https://doi.org/10.1007/s40823-021-00067-y

Hoffrén, R., Lamelas, M.T., de la Riva, J., Domingo, D., Montealegre, A.L., García-Martín, A. and Revilla, S., 2023. Assessing GEDI-NASA system for forest fuels classification using machine learning techniques. International Journal of Applied Earth Observation and Geoinformation, 116, p.103175. https://doi.org/10.1016/j.jag.2022.103175.

Jain, P., Coogan, S.C., Subramanian, S.G., Crowley, M., Taylor, S. and Flannigan, M.D., 2020. A review of machine learning applications in wildfire science and management. *Environmental Reviews*, *28*(4), pp.478-505. dx.doi.org/10.1139/er-2020-0019

Jones, M.W., Abatzoglou, J.T., Veraverbeke, S., Andela, N., Lasslop, G., Forkel, M., Smith, A.J., Burton, C., Betts, R.A., van der Werf, G.R. and Sitch, S., 2022. Global and regional trends and drivers of fire under climate change. *Reviews of Geophysics*, *60*(3), p.e2020RG000726.

Kashparov, V., Kirieiev, S., Yoschenko, V., Levchuk, S., Holiaka, D., Zhurba, M., Bogdan, L., Vyshnevskyi, D. and Oughton, D.H., 2024. Assessment of exposures to firefighters from wildfires in heavily contaminated areas of the Chornobyl

Exclusion Zone. Journal of Environmental Radioactivity, 274, p.107410. https://doi.org/10.1016/j.jenvrad.2024.107410.

Key, C.H. and Benson, N.C., 2006. Landscape assessment (LA). FIREMON: Fire effects monitoring and inventory system, 164, pp.LA-1.

Knapp, E.E., Lydersen, J.M., North, M.P. and Collins, B.M., 2017. Efficacy of variable density thinning and prescribed fire for restoring forest heterogeneity to mixed-conifer forest in the central Sierra Nevada, CA. Forest Ecology and Management, 406, pp.228-241. https://doi.org/10.1016/j.foreco.2017.08.028.

Kolden, C.A., Lutz, J.A., Key, C.H., Kane, J.T. and Van Wagtendonk, J.W., 2012. Mapped versus actual burned area within wildfire perimeters: characterizing the unburned. Forest Ecology and Management, 286, pp.38-47. https://doi.org/10.1016/j.foreco.2012.08.020.

Krawchuk, M.A., Haire, S.L., Coop, J., Parisien, M.A., Whitman, E., Chong, G. and Miller, C., 2016. Topographic and fire weather controls of fire refugia in forested ecosystems of northwestern North America. Ecosphere, 7(12), p.e01632. https://doi.org/10.1002/ecs2.1632.

Kvålseth, T.O. (1989) 'Note on Cohen's kappa,' Psychological Reports, 65(1), pp. 223–226. https://doi.org/10.2466/pr0.1989.65.1.223.

Lechner, A.M., Foody, G.M. and Boyd, D.S., 2020. Applications in remote sensing to forest ecology and management. One Earth, 2(5), pp.405-412. https://doi.org/10.1016/j.oneear.2020.05.001.

Liang, L., Shang, R., Chen, J. M., Xu, M., & Zeng, H. (2023). Improved estimation of the underestimated GEDI footprint LAI in dense forests. *Geo-Spatial Information Science*, 1–16. https://doi.org/10.1080/10095020.2023.2286377

Lipton, Z.C., Elkan, C. and Narayanaswamy, B., 2014. Thresholding classifiers to maximize F1 score. *arXiv preprint arXiv:1402.1892*.

Li, H., Li, X., Kato, T., Hayashi, M., Fu, J. and Hiroshima, T., 2024. Accuracy Assessment of GEDI Terrain Elevation, Canopy Height, and Aboveground Biomass Density Estimates in Japanese Artificial Forests. *Science of Remote Sensing*, p.100144. https://doi.org/10.1016/j.srs.2024.100144

Liu, C. and Wang, S., 2022. Estimating tree canopy height in densely forest-covered mountainous areas using GEDI spaceborne full-waveform data. ISPRS Annals of the Photogrammetry, Remote Sensing and Spatial Information Sciences, 1, pp.25-32. https://doi.org/10.5194/isprs-annals-v-1-2022-25-2022.

Mackey, B., Lindenmayer, D., Norman, P., Taylor, C. and Gould, S., 2021. Are fire refugia less predictable due to climate change?. Environmental Research Letters, 16(11), p.114028. https://doi.org/10.1088/1748-9326/ac2e88.

Masson, O., Romanenko, O., Saunier, O., Kirieiev, S., Protsak, V., Laptev, G., Voitsekhovych, O., Durand, V., Coppin, F., Steinhauser, G. and de Vismes Ott, A., 2021. Europe-wide atmospheric radionuclide dispersion by unprecedented wildfires in the chernobyl exclusion zone, April 2020. Environmental Science & Technology, 55(20), pp.13834-13848. https://doi.org/10.1021/acs.est.1c03314.

Matsala, M., Bilous, A., Myroniuk, V., Holiaka, D., Schepaschenko, D., See, L. and Kraxner, F., 2021. The return of nature to the Chernobyl Exclusion Zone:

increases in forest cover of 1.5 times since the 1986 disaster. Forests, 12(8), p.1024. https://doi.org/10.1021/acs.est.1c03314.

Matsala, M., Myroniuk, V., Borsuk, O., Vishnevskiy, D., Schepaschenko, D., Shvidenko, A., Kraxner, F. and Bilous, A., 2023. Wall-to-wall mapping of carbon loss within the Chornobyl Exclusion Zone after the 2020 catastrophic wildfire. Annals of Forest Science, 80(1), p.26. https://doi.org/10.1186/s13595-023-01192-w.

Matsala, M., Odruzhenko, A., Hinchuk, T., Myroniuk, V., Drobyshev, I., Sydorenko, S., Zibtsev, S., Milakovsky, B., Schepaschenko, D., Kraxner, F. and Bilous, A., 2024. War drives forest fire risks and highlights the need for more ecologically-sound forest management in post-war Ukraine. *Scientific reports*, *14*(1), p.4131. https://doi.org/10.1038/s41598-024-54811-5.

Maxwell, A.E., Farhadpour, S. and Das, S., 2024. geodl: An R package for geospatial deep learning semantic segmentation using torch and terra.

Meigs, G.W., Dunn, C.J., Parks, S.A. and Krawchuk, M.A., 2020. Influence of topography and fuels on fire refugia probability under varying fire weather conditions in forests of the Pacific Northwest, USA. Canadian Journal of Forest Research, 50(7), pp.636-647. https://doi.org/10.1139/cjfr-2019-0406

Meigs, G.W. and Krawchuk, M.A. (2018) 'Composition and Structure of Forest Fire Refugia: What Are the Ecosystem Legacies across Burned Landscapes?,' Forests, 9(5), p. 243. https://doi.org/10.3390/f9050243.

Meddens, A.J., Kolden, C.A. and Lutz, J.A., 2016. Detecting unburned areas within wildfire perimeters using Landsat and ancillary data across the northwestern United States. Remote Sensing of Environment, 186, pp.275-285. https://doi.org/10.1016/j.rse.2016.08.023.

Meddens, A.J., Kolden, C.A., Lutz, J.A., Smith, A.M., Cansler, C.A., Abatzoglou, J.T., Meigs, G.W., Downing, W.M. and Krawchuk, M.A., 2018. Fire refugia: what are they, and why do they matter for global change?. BioScience, 68(12), pp.944-954. https://doi.org/10.1093/biosci/biy103.

Moreau, G., Chagnon, C., Achim, A., Caspersen, J., D'Orangeville, L., Sánchez-Pinillos, M. and Thiffault, N., 2022. Opportunities and limitations of thinning to increase resistance and resilience of trees and forests to global change. *Forestry*, *95*(5), pp.595-615. https://doi.org/10.1093/forestry/cpac010

Myroniuk, V., Zibtsev, S., Bogomolov, V., Goldammer, J.G., Soshenskyi, O., Levchenko, V. and Matsala, M., 2023. Combining Landsat time series and GEDI data for improved characterization of fuel types and canopy metrics in wildfire simulation. Journal of Environmental Management, 345, p.118736. https://doi.org/10.1016/j.jenvman.2023.118736.

Nowacki, G.J. and Abrams, M.D., 2008. The demise of fire and "mesophication" of forests in the eastern United States. *BioScience*, *58*(2), pp.123-138.

Pausas, J.G., Bladé, C., Valdecantos, A., Seva, J.P., Fuentes, D., Alloza, J.A., Vilagrosa, A., Bautista, S., Cortina, J. and Vallejo, R., 2004. Pines and oaks in the restoration of Mediterranean landscapes of Spain: new perspectives for an old practice—a review. *Plant ecology*, *171*, pp.209-220. https://doi.org/10.1023/B:VEGE.0000029381.63336.20

Penner, M., D.G. Pitt, and M.E. Woods. 2013. “Parametric vs. Nonparametric LiDAR Models for Operational Forest Inventory in Boreal Ontario.” *Canadian Journal of Remote Sensing* 39 (5): 426–43. https://doi.org/10.5589/m13-049

Proença, V., Pereira, H.M. and Vicente, L., 2010. Resistance to wildfire and early regeneration in natural broadleaved forest and pine plantation. *Acta Oecologica*, *36*(6), pp.626-633. https://doi.org/10.1016/j.actao.2010.09.008.

QGIS, n.d. Changelog for QGIS 3.28. Available at: https://www.qgis.org/en/site/forusers/visualchangelog328/index.html [Accessed 12 March 2024].

Robinson, N.M., Leonard, S.W., Bennett, A.F. and Clarke, M.F., 2014. Refuges for birds in fire-prone landscapes: the influence of fire severity and fire history on the distribution of forest birds. Forest Ecology and Management, 318, pp.110-121. https://doi.org/10.1016/j.foreco.2014.01.008.

Stephens, S.L., Burrows, N., Buyantuyev, A., Gray, R.W., Keane, R.E., Kubian, R., Liu, S., Seijo, F., Shu, L., Tolhurst, K.G. and Van Wagtendonk, J.W., 2014. Temperate and boreal forest mega-fires: characteristics and challenges. Frontiers in Ecology and the Environment, 12(2), pp.115-122. https://doi.org/10.1890/120332.

UNCG, 2023. *Z 24 liutoho v zoni vidchuzhennia vyhorilo ponad 22000 ha: naslidky okupatsii prodovzhuiut zavdavaty shkody dovkilliu*. [online] Available at: https://uncg.org.ua/z-24-liutoho-v-zoni-vidchuzhennia-vyhorilo-ponad-22000-ha-naslidky-okupatsii-prodovzhuiut-zavdavaty-shkody-dovkilliu/ [Accessed 11 July 2024].

USDA Forest Service (n.d.) *Carpinus caroliniana*. Available at: https://www.fs.usda.gov/database/feis/plants/tree/carcar/all.html#:~:text=FIRE%20EFFECTS,-SPECIES%3A%20Carpinus%20caroliniana&text=IMMEDIATE%20FIRE%20EFFECT%20ON%20PLANT,of%20a%20white%20oak%20(Q. (Accessed: 10 June 2024)

Vallejo, V.R., Arianoutsou, M., Moreira, F. (2012). Fire Ecology and Post-Fire Restoration Approaches in Southern European Forest Types. In: Moreira, F., Arianoutsou, M., Corona, P., De las Heras, J. (eds) Post-Fire Management and Restoration of Southern European Forests. Managing Forest Ecosystems, vol 24. Springer, Dordrecht. https://doi.org/10.1007/978-94-007-2208-8_5

What are the best Landsat spectral bands for use in my research? | U.S. Geological Survey (2024). https://www.usgs.gov/faqs/what-are-best-landsat-spectral-bands-use-my-research.

Whelan, R., 1995. The Ecology of Fire. Cambridge University Press, Cambridge, England.

World Economic Forum, 2021. This is how much carbon wildfires have emitted this year (2021). Available at: https://www.weforum.org/agenda/2021/12/siberia-america-wildfires-emissions-records-2021/ [Accessed 4 June 2024].

Xi, Z.; Xu, H.; Xing, Y.; Gong, W.; Chen, G.; Yang, S. Forest Canopy Height Mapping by Synergizing ICESat-2, Sentinel-1, Sentinel-2 and Topographic Information

Based on Machine Learning Methods. Remote Sens. 2022, 14, 364. https://doi.org/10.3390/rs1402036

Yoschenko, V.I., Kashparov, V.A., Protsak, V.P., Lundin, S.M., Levchuk, S.E., Kadygrib, A.M., Zvarich, S.I., Khomutinin, Y.V., Maloshtan, I.M., Lanshin, V.P. and Kovtun, M.V., 2006. Resuspension and redistribution of radionuclides during grassland and forest fires in the Chernobyl exclusion zone: part I. Fire experiments. Journal of Environmental Radioactivity, 86(2), pp.143-163. https://doi.org/10.1016/j.jenvrad.2005.08.003.

Zhuravel, O.A., 2021. Assessment of the wildfires impact on the ecosystems of the Chornobyl Exclusion Zone (Doctoral dissertation, National Aviation University).

Zibtsev, S.V., Goldammer, J.G., Robinson, S. and Borsuk, O.A., 2015. Fires in nuclear forests: silent threats to the environment and human security. Unasylva, 66(243/244), p.40. https://www.proquest.com/openview/8747bb308c24eb1d313a3a23c1c8405d/1?pq-origsite=gscholar&cbl=2037532.

Zymaroieva A, Kolomiychuk V, Fedoniuk T, Goncharenko I, Borsuk O, Melnychuk T, Svenning JC. Post-fire recovery of vegetation in the Chornobyl Radiation and Ecological Biosphere Reserve. International Journal of Environmental Studies. 2024 Jan 2;81(1):489-509. https://doi.org/10.1080/00207233.2023.2287345.

Popular science summary

Escaping the flames: How nature finds a safe haven in the Chornobyl Exclusion Zone

Forest fires are an important driver of ecosystem dynamics in boreal and temperate forests. However, climate change is making these fires intense and difficult to control. As for the Chornobyl Exclusion Zone (ChEZ), forest fires interact with landscape in different ways, but our focus is on the factors in the surroundings of these forest areas, determining whether they survive or burned.

In May 2022, a fire in the southeastern part of ChEZ, sparked by the Russian invasion of Ukraine, burned an area of 14,000 hectares, including plantations established after a similar fire in 1992. Despite the destruction, some forest patches survived. Our research identifies the role of surrounding patches in influencing the fire behaviour in burned and unburned patches. We believe that diverse forest structures and fuel breaks near these forests could contribute to. Through this research, we aim to uncover what makes forests resillient and how this knowledge can be used to design production forests in the future.

Acknowledgements

I would like to acknowledge my supervisor Maksym Matsala and co-supervisor Igor Drobyshev for their immense support and supervision in finishing the research work. I am happy I am not only learned so much from them, but also built friendly relationships. I want to say thank you to Erlita, who was there for me for everything and giving me the strength to keep going. I thank to Shakhera, who supported me and assisted me with any academic needs. I say thank you to my best friend, Ajin who backed me up in any situation regardless the difficulty. I am thanking to Sana, Darshan, Siddhardh, Shraddha, Khudirat, and Janneke for supporting me throughout my academic journey. I am grateful to all of my friends of SUFONAMA (Sustainable Forest and Nature Management) and SLU's Euroforester (2023/24) program for making my academic journey colourful. I want to express my gratitude to my professors and, program coordinators and related persons of EMJMD in SUFONAMA program under the European Commission for giving me a life-changing opportunity to study at SLU (Swedish University of Agricultural Sciences).

Publishing and archiving

Approved students' theses at SLU are published electronically. As a student, you have the copyright to your own work and need to approve the electronic publishing. If you check the box for **YES**, the full text (pdf file) and metadata will be visible and searchable online. If you check the box for **NO**, only the metadata and the abstract will be visible and searchable online. Nevertheless, when the document is uploaded it will still be archived as a digital file. If you are more than one author, the checked box will be applied to all authors. You will find a link to SLU's publishing agreement here:

- https://libanswers.slu.se/en/faq/228318.

☒ YES, I/we hereby give permission to publish the present thesis in accordance with the SLU agreement regarding the transfer of the right to publish a work.

☐ NO, I/we do not give permission to publish the present work. The work will still be archived and its metadata and abstract will be visible and searchable.